Engineering Structures 303 (2024) 117573

Contents lists available at ScienceDirect

Engineering Structures

journal homepage: www.elsevier.com/locate/engstruct

# Lightly reinforced concrete walls in formwork blocks for the combined seismic and energy retrofit of masonry structures

Silvia Caprili [a,*], Giuseppe Chellini [a], Francesca Mattei [a], Walter Salvatore [a], Gemma Simonetti [b], Massimo Badalassi [c]

[a] Department of Civil and Industrial Engineering, University of Pisa, Largo L. Lazzarino 1, 56122 Pisa, Italy
[b] Technical instructor, Municipality of Chiusdino, Piazza del Plebiscito, 2, 53012 Chiusdino, Siena, Italy
[c] S.I.T.A. Engineering s.r.l., Pisa, Italy

ARTICLE INFO

*Keywords:*
Seismic retrofit
Lightly reinforced concrete walls
Formwork blocks
Energy refurbishment
Seismic performance

ABSTRACT

In recent years the interest is arising towards systems for the combined structural and energy retrofit of existing structures. In the present paper a retrofit system consisting in a lightly reinforced concrete wall realized within formwork blocks in expanded clay is proposed; the shape of the blocks allows the introduction of an insulation layer with high isolation capacity. The system is conceived to work in parallel with the existing masonry structure: the realized reinforced concrete wall acts as a shear panel devoted to carry on the horizontal seismic actions, being the existing masonry walls in still in force to sustain vertical loads. Opportune connections are realized in correspondence of the horizontal floors' levels to transfer only the horizontal actions. Conceptual design, together with application to a real case study existing masonry building that allows to size and detail the panel, is presented. The results of experimental tests with horizontal forces on the proposed system are shown, as well as the calibration of a simple model able to estimate its dissipative performance as function of structural details and material properties.

## 1. Introduction

Unreinforced masonry buildings represent the majority of the existing Italian residential heritage; according to ISTAT database [1], the masonry typology is the widest diffused over the Country, i.e. 57% are masonry structures against the only 29% of reinforced concrete (RC) one and the 13% of buildings realized with different materials and construction techniques (steel, steel-composite, mixed masonry/reinforced concrete, etc.). About the 84% of the residential buildings was realized between the end of the 2nd World War and the 1990 s, the 15% before 1919, the 11% in the period 1919÷1945 and only the 14% after 1990: being therefore mostly realized before the enactment of specific design rules to prevent (or limit) damages due to earthquakes, many structural deficiencies exist concerning the performance against horizontal actions. The situation gets even worst if we consider that such buildings are approaching the end of their nominal life and the need of relevant retrofit interventions. Recent and past seismic events (L'Aquila 2009, Umbria-Marche 1997, Centro-Italia 2016) evidenced the high seismic vulnerability of existing masonry buildings, with severe damages in terms of human losses, partial or global failures and loss of artistic values, hard to be recovered due to the strong economic effort required. Many solutions are proposed for the seismic retrofit of existing masonry buildings, spacing from traditional techniques such as the use of chains, masonry strengthening, etc. to the introduction of innovative base-isolation systems [2,3] or of damping devices [4,5,6], these last ones often difficult to be applied considering the need of preserving the original nature of the artefact. Recently, in the wide European scenario, the interest is arising in the development of combined solutions able to improve, together with the structural performance, the energy consumptions. Improving the energy capacity has become essential to match the EU Commission's aim of achieving a highly efficient and decarbonised building stock by 2050 [7]: after a long period where improving the seismic behaviour and reducing the energy consumptions were addressed separately, the Energy Performance of Buildings Directive [8] planned a common framework including energy performance strategies, reduction of fire safety and seismic risk prevention for buildings, highlighting how the energy refurbishment may be lost when earthquakes happen in lack of adequate structural interventions, and

* Corresponding author.
*E-mail address:* silvia.caprili@unipi.it (S. Caprili).

https://doi.org/10.1016/j.engstruct.2024.117573
Received 13 September 2023; Received in revised form 31 December 2023; Accepted 23 January 2024

vice-versa [7–11]. Pohoryles et al. [9] proved the connection between the high values of $CO_2$ emission and energy waste and the wide percentage of buildings elder than 50 years old, characterized by inadequate energy performance.

Several solutions exist able to join the energy refurbishment and the seismic retrofit of existing masonry buildings. To mention only few, Bournas [12] proposed the combination of a Textile Reinforced Mortar (TRM) jacketing and thermal insulation materials applied to both masonry and RC buildings. Borri et al. [13] studied the shear performance of wall panels reinforced with Glass Fibre Reinforced Polymer (GFRP) meshes embedded into lime-based mortars, able to join benefit in terms of both structural performance and thermal conductivity. Baek et al. [14] proposed a hybrid solution for the seismic and energy retrofit consisting of prefabricated Textile Reinforced Concrete (TRC) panels including capillary tubes for the energy upgrading, the so-called Textile Capillary Tube Panels (TCPs). The systems proposed by Facconi et al. [15], Longo et al. [16], Gkournelos et al. [17] also deserve to be mentioned, applied even to buildings characterized by high artistic value. Other possibilities consist in the adoption of exoskeletons, i.e. the realization of two separate structures coupled with non-dissipative connections aiming to achieve an in-plane rigid behaviour with separate response to seismic actions [18–21].

The present work deals with the development of an innovative solution for the combined seismic and energy retrofit of existing structures, preliminary conceived for unreinforced masonry buildings. The general idea is the introduction of lightly RC walls realized by casting in expanded-clay formworks blocks, working in parallel with the existing building. The geometry of the blocks was studied to allow, besides the concrete cast, the introduction of a Neopor® layer for the energy refurbishment. A single intervention is then able to provide seismic (thanks to the RC panels) and energy retrofit (thanks to the insulated layer). The system was proposed in the framework of a scientific collaboration between University of Pisa and PAVER Costruzioni S.p.A. who developed, in the past, a similar system for the realization of new buildings [22,23]. The overall research project joints experimental tests and numerical simulations aiming to provide practical indications to designers for the application of the proposed system. The present paper is an excerpt of the whole work dealing with the conceptual development of the retrofit system, its preliminary design and the numerical application to a representative case-study building to prove its structural and energy benefit. The experimental investigation of the stand-alone panel under lateral load excitation is also presented, being fundamental to assess its impact on the existing building. Even if the system is similar to the one already adopted for new constructions, the employment of a reduced thickness needs to perform accurate investigations to validate the reliability of current indications [22,23]. A further experimental phase, concerning the application of the retrofit panel to the existing wall under lateral/seismic actions is actually ongoing and will be the topic of a following paper.

## 2. Design and application of the proposed retrofit system

### 2.1. Conceptual design

The proposed retrofit system consists in a lightly RC wall realized using expanded-clay formwork blocks working in parallel to the existing masonry structure. The retrofit panel is connected to the masonry walls only in correspondence of the horizontal storeys and owns an individual foundation system. The so-realized RC shear wall acts therefore as a bracing system facing horizontal seismic actions, while the vertical loads are carried out by the existing structure. It is applied all around the building perimeter, realizing a sort of exoskeleton able to improve the energy performance and the in-plane seismic behaviour and to prevent the out-of-plane mechanisms of the existing masonry walls.

The thickness of formwork blocks is 235 mm: it allows the introduction of an internal concrete cast, reinforced vertically and horizontally, and the interposition of the isolation layer (Fig. 1). The proposed system retraces the concept of the BioPLUS® one, widely tested in 2010 and whose deep numerical analyses allowed the elaboration of proper design indications [23]. The application, the dimensions and the structural performance of the proposed retrofit system however differ from BioPLUS® and require the elaboration of specific design indications when applied to existing structures. The geometry and disposition of the formwork blocks, following alternated rows, and the presence of internal horizontal ribs (Fig. 1) make the concrete cast to be not continuous, nor horizontally neither vertically. Tùhe reinforcement layout consists in a single layer of longitudinal rebars and in a double rebars' layer in the transversal direction, respecting the geometrical ratio limitation (i.e. $\rho_{min}$ equal to 0.20%) required for RC walls [24,25].

The connection between the retrofit panel and the existing masonry wall is realized in correspondence of the existing RC beams of the horizontal storey slabs (if present); steel L-bent connectors suitably sized, spaced and embedded in the RC beams through resins' injections can be used. If the concrete curb lacks, an opportune connection system shall be organized using, for instance, additional supporting steel structures. This is, for instance, the case of masonry buildings realized with timber storeys, with beams resting directly upon the walls: in such cases, steel beams (L section) can be used to recreate, all along the perimeter, the box behaviour. The retrofit system is then fixed to the steel curb through adequate connectors. The economic effort, excluding the costs of the steel material, are comparable in the two different situations. The foundation system shall be designed to transfer the seismic actions to the ground: if the existing foundation is large enough and can resist the horizontal loads, the retrofit panels can be directly lie on it; otherwise, new RC beams, adjacent and anchored to the existing ones, shall be realized. This last case will require, undeniably, a higher economic effort due to excavation, formworks, concrete casting and reinforcements, etc. The limited thickness of the proposed retrofit system, however, makes highly probable that the existing foundation will be able to host the retrofit panel. Preliminary in-situ investigations on the existing building are required as in the case of any other retrofit intervention.

From an operational point of view, the layer of polystyrene insulating material is introduced within the formwork blocks during the processing phase, so that blocks are ready to be assembled for the following concrete casting, that will fill the remaining portion with nominal thickness equal to 100 mm. The concrete casting shall be realized after the introduction of suitable sized vertical and horizontal reinforcements. In case of presence of an existing foundation able to host the retrofit panel (for dimensions and bearing capacity) injection grouting will be used to anchor adequately sized connectors able to join the retrofit panels to the existing foundation. On the contrary, if the realization of a new specific foundation beam is needed, the first steps will be the excavation, the positioning of adequate formworks and the concrete casting, paying attention to the pre-disposition of connection rebars between the foundation beams and the retrofit panels. After the realization of the perimeter retrofit panels and the casting of the concrete curbs, connections will be realized at the horizontal floor levels using, for instance, adequate steel L-bent connectors or, alternatively, chemical injection anchors opportunely sized and spaced along the curb.

### 2.2. Preliminary design of the retrofit system

The preliminary design of the retrofit panel was performed by considering its application to existing masonry walls with different geometry, providing an initial estimation of the rebars' layout (diameter, spacing, amount) and of the following design actions. The existing walls were supposed to belong to a typical unreinforced masonry two-storey building made up of solid double-headed bricks with clay mortar and thickness equal to 25 cm. The choice of the thickness of the existing masonry walls depended upon the in-depth analysis of the Italian building heritage of the XX century, being the most representative

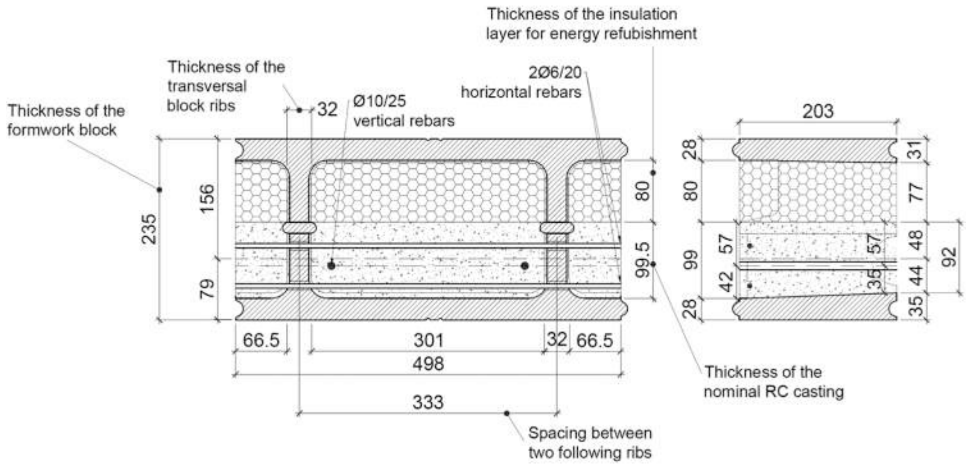


**Fig. 1.** Typical formwork blocks used for the realization of the retrofit panels.

masonry typologies the full-brick masonry one (single block dimensions 250 mm × 125 mm x 55 mm used double headed or positioned in thickness) and the hollow DoppioUNI one, with comparable dimensions. The horizontal storey was considered to weight upon the existing wall. The mechanical properties of the existing structure were derived from Circ.7/2019 [26].

The influence of the slenderness ratio (defined as $L/H$ ratio, being $H$ and $L$ respectively the height and the length of the panel) was analysed being relevant for the out-of-plane performance in case of reduced wall thickness (i.e. like the present situation). Considering the blocks' geometry (Fig. 1) and the need of introducing the isolation layer for the energy refurbishment, a concrete cast with nominal thickness 100 mm was realized; concrete class C25/30 (S4) and rebars B450C were used.

Following, initially, the indications provided by [23], an equivalence was made between the non-continuous concrete cast realized within the blocks and a continuous RC wall of equivalent thickness ($t_{eq}$) provided by Eq. (1), being $L$ the length of the panel and $A_{eff}$ the total concrete area in correspondence of the transversal section.

$$t_{eq} = A_{eff}/L \quad (1)$$

The equivalent thickness of the retrofit panel (nominal casting of 100 mm) was equal to 82.89 mm.

The formulation proposed by [23], adopted for the pre-design, was validated by the experimental tests presented in the following, necessary operation since geometry and loading conditions differ from the typical ones of new buildings. Refined numerical fibre nonlinear models were realized using different software, including DIANA® - specific for masonry structures and SAP2000® - simpler in application especially insight of providing practical design and modelling indications for engineers. Results were similar, since the general assumptions made for the constitutive laws of the materials and connectors were the same. Bidimensional shell elements were used for both the existing masonry wall and the retrofit panel. Rigid links at storeys' level spaced by 20 cm to simulate the transfer of the only horizontal actions from the existing wall to the retrofit panel. At ultimate limit state, the stiffness of masonry and concrete elements was reduced to account for cracking phenomena [27,28].

Loads' evaluation was performed according to [27]; the material density of the existing masonry was equal to 18 kN/m$^3$, the permanent loads of the retrofit system amounted to 3.775 kN/m$^2$ (including the formwork blocks, the concrete cast and the isolation layer) and, for horizontal storeys, $G_1$, $G_2$ and $Q_k$ were assumed equal to 3.0 kN/m$^2$, 3.0 kN/m$^2$ and 2.0 kN/m$^2$. The design seismic action was evaluated with reference to the building from which the panels were extracted, considering a nominal life ($V_N$) equal to 50 years and use class ($C_U$) II, Pistoia as location, soil foundation category C and topographic category $T_1$. A behaviour factor equal to 1.50 was assumed, considering the retrofitted structure a mixed masonry/concrete building and actually lacking further information.

The two conditions before (existing wall) and after (existing wall+ RC panel in formwork blocks) the retrofit application were compared in terms of stiffness, shear action, seismic masses, etc. using the results of a linear dynamic analysis with response spectrum. Table 1 shows the values of $S_d(T_1)$ - spectral acceleration corresponding to $T_1$, $W_{ed}$ - participating mass and $V_{ed}$ – resulting shear force.

The increase of the stiffness of the whole system was evident, with the following decrease of the vibration period shifting from 0.299 s to 0.118 s (in case of $L/H$ 1:1). The demand acting on both the existing and the retrofit panels was evaluated in terms of bending, axial force and shear actions. For the determination of the capacity, the formulations provided by current standards for masonry and lightly RC walls were used [24,27]. Rebars' layout of the retrofit panel resulted in horizontal rebars 2ϕ6/20 (two layers) and vertical rebars ϕ10/25 (single layer) symmetrically positioned with respect to the panel's section. After retrofit, as expected, about all the shear actions were carried out by the retrofit panels, unloading the existing masonry panels that become, therefore, secondary elements (the shear demand decreased from 76.2 kN to 10.9 kN in case of $L/H$ (1:1), Table 2). The decrease of the flexural demand was also appreciated.

Table 2 shows the results of bending and (sliding) shear assessment for the different $L/H$ ratios.

The connection between the retrofit panel and the existing wall was designed using L-rebars ϕ12/30 grouted through epoxy resins. The assessment of the connection system accounted for two different criteria, i.e. [24] for shear action at the interface with concrete cast and [29] for chemical anchors in concrete. Assuming the use of 3ϕ12 per linear meter

**Table 1**
Main results of linear static analysis on considered elements in terms of seismic mass and shear action (demand actions). Lev.I: 3.0 m, Lev.II: 6.0 m.

| | | *L/H* (1:1) | | *L/H* (2:1) | | *L/H* (1:2) | |
|---|---|---|---|---|---|---|---|
| | | 3.0 × 3.0 (2 floors) | | 6.0 × 3.0 (2 floors) | | 1.5 × 3.0 (2 floors) | |
| | | *before* | *after* | *before* | *after* | *before* | *after* |
| $T_1$ [s] | | 0.299 | 0.118 | 0.192 | 0.077 | 0.643 | 0.248 |
| $S_d(T_1)$ [g] | | 0.363 | 0.331 | 0.363 | 0.295 | 0.260 | 0.363 |
| $W_{Ed}$ [t] | Lev.II | 9.67 | 11.41 | 19.34 | 22.83 | 6.10 | 6.97 |
| | Lev.I | 11.77 | 15.26 | 23.55 | 30.52 | 7.15 | 8.89 |
| | Tot | 21.44 | 26.67 | 42.89 | 53.35 | 13.25 | 15.86 |
| $V_{Ed}$ [kN] | Lev.II | 47.43 | 51.89 | 94.85 | 92.41 | 21.32 | 34.45 |
| | Lev.I | 28.87 | 34.69 | 57.74 | 61.77 | 12.5 | 21.98 |
| | Tot | 76.3 | 86.58 | 152.59 | 154.19 | 33.82 | 56.43 |

**Table 2**
Results of safety assessment on the considered masonry walls before and post retrofit.

| L/H | Section | $N_{Ed}$ [kN] | $M_{Ed}$ [kNm] | $V_{Ed}$ [kN] | $M_{Ed}/M_{Rd}$ | $V_{Ed}/V_{Rd}$ (sliding) | $V_{Ed}/V_{Rd}$ | Condition |
|---|---|---|---|---|---|---|---|---|
| (1:1) | Bottom | 251.0 | 360.3 | 76.2 | 1.46 | 2.07 | 0.40 | Before retrofit |
| | Top | 212.0 | 155.4 | 76.2 | 0.69 | 1.14 | 0.43 | |
| | Bottom | 253.1 | 52.3 | 10.9 | 0.21 | 0.13 | 0.06 | After retrofit |
| | Top | 214.1 | 23.0 | 10.9 | 0.10 | 0.14 | 0.06 | |
| (2:1) | Bottom | 511.9 | 745.2 | 152.5 | 0.50 | 1.05 | 0.40 | Before retrofit |
| | Top | 439.9 | 363.9 | 152.5 | 0.39 | 0.96 | 0.42 | |
| | Bottom | 516.0 | 102.9 | 17.8 | 0.10 | 0.11 | 0.05 | After retrofit |
| | Top | 444.0 | 58.3 | 17.8 | 0.06 | 0.11 | 0.05 | |
| (1:2) | Bottom | 165.1 | 159.6 | 33.8 | 2.34 | N.V. | 0.49 | Before retrofit |
| | Top | 147.1 | 75.0 | 33.8 | 1.14 | 1.07 | 0.51 | |
| | Bottom | 166.3 | 33.9 | 7.0 | 0.50 | 0.15 | 0.10 | After retrofit |
| | Top | 148.3 | 16.3 | 7.0 | 0.25 | 0.16 | 0.11 | |

(B450C), the resulting shear resistance (31.4 kN/m) satisfied the demand coming from numerical simulations (17.5 kN/m).

Buckling analyses were performed to assess the out-of-plane behaviour of the retrofit panel and the need of accounting for II order effects. The nominal stiffness method [24] was used, including geometric non-linearities but linear modelling materials, accounting for reduced cracked stiffness and rebars' contribution. Conservatively, the tension-stiffening effect was neglected. The elastic stiffness of the section was evaluated through a fiber model, neglecting the concrete tensile strength and assuming, as flexural stiffness of the section for the entire development of the wall, the cracked section's one. No buckling issues were revealed for the panel; the need of accounting for II order effects was, on the other hand, highlighted in case of reduced thickness and increased panel's length, requiring in-depth solutions.

### 2.3. *Application to a representative existing masonry building*

The application of the retrofit system to a real unreinforced masonry case-study building located in Piacenza (Italy) was analysed. The general layout of the building is given by Fig. 2, with overall plan dimensions of about 14.0 m x 8.50 m and interstorey height up to 3.50 m. The masonry walls were made up of brick type 'Doppio UNI' with

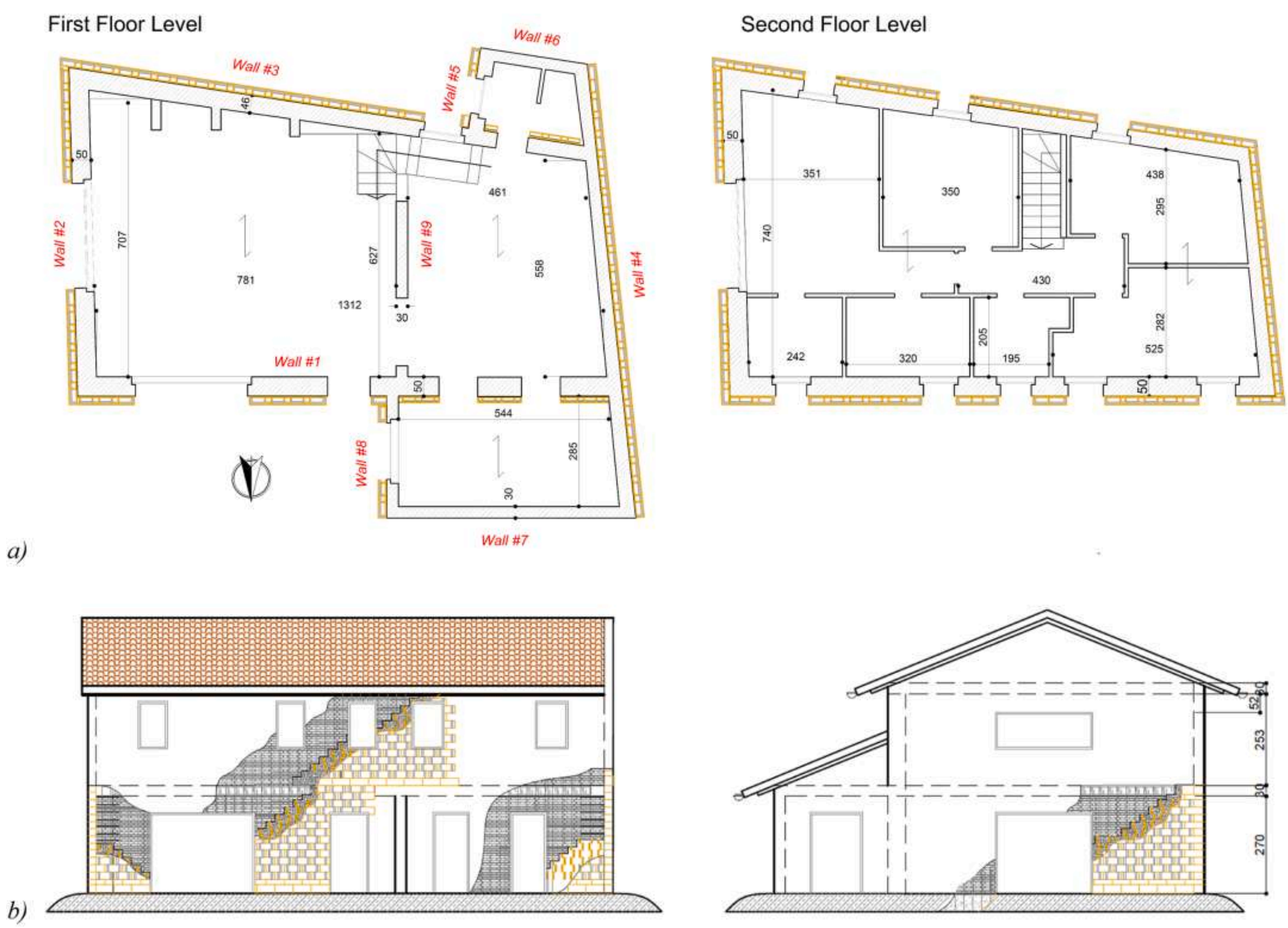


**Fig. 2.** a) Plan and b) main front view of the considered case study building with application of the proposed retrofit system.

thickness range 30÷50 cm (different dispositions of the blocks were used). Horizontal RC storeys with hollow-bricks and concrete slabs 40 mm and perimeter curbs were considered. The roof cover presented cellular reduced-height walls directly lying on the ceiling storey. The compression ($f_c$) and shear ($f_{v0}$) strength of the existing masonry were respectively equal to 345 and 20 N/cm$^2$; the elastic moduli $E$ and $G$ respectively 1500 and 500 MPa and the density 9.20 kN/m$^3$.

The analysis of the structural performance in the state-of-art condition was performed according to [27]. $G_1$ and $G_2$ permanent loads were equal to 3.0 kN/m$^2$ and 3.7 kN/m$^2$ for the interstorey slabs (1st level) and to 5.1 kN/m$^2$ and 0.6 kN/m$^2$ for the roof cover. The live loads $Q_k$ were equal to 2.0 kN/m$^2$ (1st floor level, residential building) and 1.2 kN/m$^2$ (roof cover, snow action). Seismic action was evaluated considering a nominal life ($V_N$) equal to 50 years, use class ($C_U$) II, soil category C and topographic category T$_1$. A conservative behaviour factor equal to 1.50 was assumed, lacking more detailed information about the mixed RC-masonry structure.

Results of safety checks in the state-of-the-art condition evidenced issues of the existing masonry walls towards bending and shear actions (sliding shear, mainly) in presence of seismic action, requiring therefore retrofit for masonry walls # 1, 2, 5, 6, 7, 8, 9 (Fig. 2), while no criticisms were revealed towards static combinations. The application along the whole perimeter of the retrofit system was then proposed: following the preliminary design performed at element level, and considering the entity of bending and shear demand coming from the analysis, retrofit panels (nominal thickness 100 mm, $t_{eq}$ 82.89 mm) reinforced with vertical ϕ10/25 and horizontal 2ϕ6/20 (two layers) rebars were applied (Fig. 2). Concrete class 25/30 (S4) and reinforcing steel type B450C were adopted; for the connection to the existing masonry walls, resins and mortar for grouting were employed.

The increase of the mass and of the stiffness of the existing building, whose $T_1$ shifted from 0.136 s to 0.087 s (Y-direction) and from 0.104 s to 0.073 s (X-direction) were appreciated. The decrease of the design spectral acceleration coupled to the increase of the seismic mass caused an overall 10% increase of the shear action was achieved (i.e. from 622 to 682 kN in X direction, and from 628 to 701 kN in Y direction). Safety checks in the post-retrofit condition (i.e. bending, axial force, shear accounted for both masonry walls and the equivalent lightly RC walls) were performed according to current standards. As a consequence of the D/C ratios higher than 1.0 in correspondence of wall #2 and of the corner portion between walls #1 and #2, to ensure the overall satisfaction of safety checks, an increased rebars' amount was introduced, i.e. additional ϕ14/25 (vertical) and 2ϕ8/20 (horizontal). Fig. 3 shows an example of the proposed retrofit panel and of its application to the masonry wall.

Although the present work deals with the analysis of the structural benefit when the proposed system is applied to existing masonry walls, it shall be marked that its application even allows a relevant improvement of thermal performance of the existing masonry wall. For instance, when applied to the case study building, the thermal transmittance $U$ of the external wall can reduce from the value of 1.32 W/m$^2$K (pre-application) to the value of 0.30 W/m$^2$K (post-application) ( Table 3).

## 3. The experimental test campaign

Two testing phases, focused on the performance of the single retrofit panel (Phase 1) and on the combined performance of the existing + retrofit system (Phase 2), were organized. Phase 1 included axial and

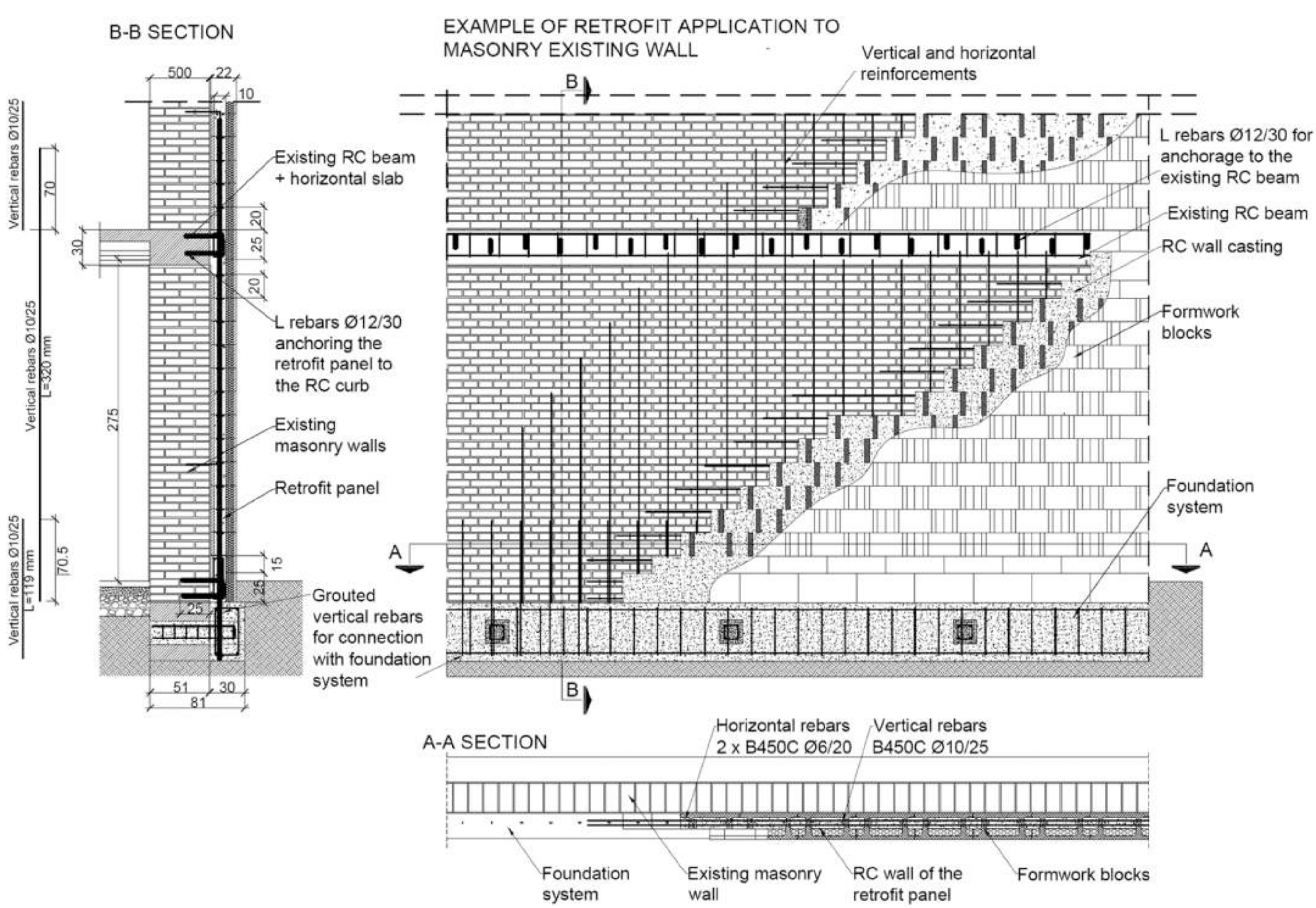


**Fig. 3.** Example of application of the retrofit system to a masonry wall (standard reinforcement, vertical and horizontal).

**Table 3**
Main results of structural analysis in terms of seismic weights and shear forces before and after the intervention.

| | | *Y-direction* | | *X-direction* | |
|---|---|---|---|---|---|
| | | *before* | *after* | *before* | *after* |
| $T_1$ [s] | | 0.136 | 0.087 | 0.104 | 0.073 |
| $S_d(T_1)$ [g] | | 0.222 | 0.192 | 0.203 | 0.183 |
| $W_{Ed}$ [t] | *Lev. II (6.00 m)* | 98.4 | 119.3 | 98.4 | 119.3 |
| | *Lev.I (3.00 m)* | 202.3 | 269.6 | 202.3 | 269.6 |
| | *Tot* | 341.5 | 445.5 | 341.5 | 445.5 |
| $V_{Ed}$ [kN] | *Liv.2 (6.00 m)* | 296.0 | 304.5 | 266.5 | 254.5 |
| | *Liv.1 (3.00 m)* | 290.5 | 336.5 | 318.5 | 382.0 |
| | *Tot* | 622.0 | 682.0 | 628.0 | 701.0 |

diagonal compression tests, tests to assess the buckling resistance of the retrofit panels against out-of-plane actions and monotonic and cyclic tests for the in-plane performance. Tests of Phase 1 are actually concluded together with their in-depth elaboration and is presented in the following paragraphs. Phase 2, actually ongoing, includes monotonic and cyclic tests on the combined system existing walls + retrofit panels, assuming two different masonry typologies representative of the majority of buildings realized more than 50 years ago (i.e. full-brick with clay mortar and hollow bricks type 'Doppio UNI'). Tests of Phase 2 are ongoing and results will be presented in a following paper. It shall be noted that results of Phase 1, hereafter presented, are necessary for the organization of Phase 2 investigations on the combined 'existing + retrofit' system, in terms of acting loads, expected forces and displacements, etc.

All tests were performed at the *Laboratorio Ufficiale per le Esperienze sui Materiali da Costruzione* of Pisa University; the specimens, as well as the other components required for the setup and tests' execution were provided by Paver Costruzioni s.r.l .

## 3.1. Compression and diagonal compression preliminary tests

### 3.1.1. Design of the specimens

Panels for monotonic axial compression load tests were about 100 cm x 100 cm x 23.5 cm ( Fig. 4a and Fig. 5a), consisting of 5 alternated rows of formwork blocks; the reinforcements' layout was widespread as possible. Flat horizontal faces were realized to ensure the perpendicular distribution of the axial load on the cross-section area. Two steel plates were introduced at the top and the bottom of the panel, together with leveling Teflon sheets to optimize load redistribution.

Specimens for diagonal compression tests were about 142 cm x 142 cm x 23.5 cm (square specimens), consisting in 7 alternated rows of formwork blocks (Fig. 4b and Fig. 5b). The horizontal reinforcements (2ϕ6/20) were welded at the ends to small steel plates (70×50×6 mm); for the vertical reinforcements (1ϕ10/25), plates 40×50×6 mm were used. To assure the load being applied centered with respect to the concrete wall, two opposite corners of the sample were realized without the formwork and the isolation layer and two 'steel corners' were introduced in adherence to the concrete wall, interposing a Teflon layer for leveling the surfaces. To limit the deformations in proximity of the corners, the first rib of the formwork block, facing the corner, was also removed.

### 3.1.2. Test setup

In case of axial compression tests, a rigid steel beam allowed the load's uniform redistribution on the specimens. The ultimate load ($F_{max}$) was measured; vertical and horizontal displacement transducers (LVDT) with measuring length range 0÷200 mm were used for deformations. The continuous acquisition of loads and displacements allowed to determine the stress-strain diagrams and the corresponding ultimate compression strength of the samples. The load was applied in three following steps till the achievement of half of the expected maximum

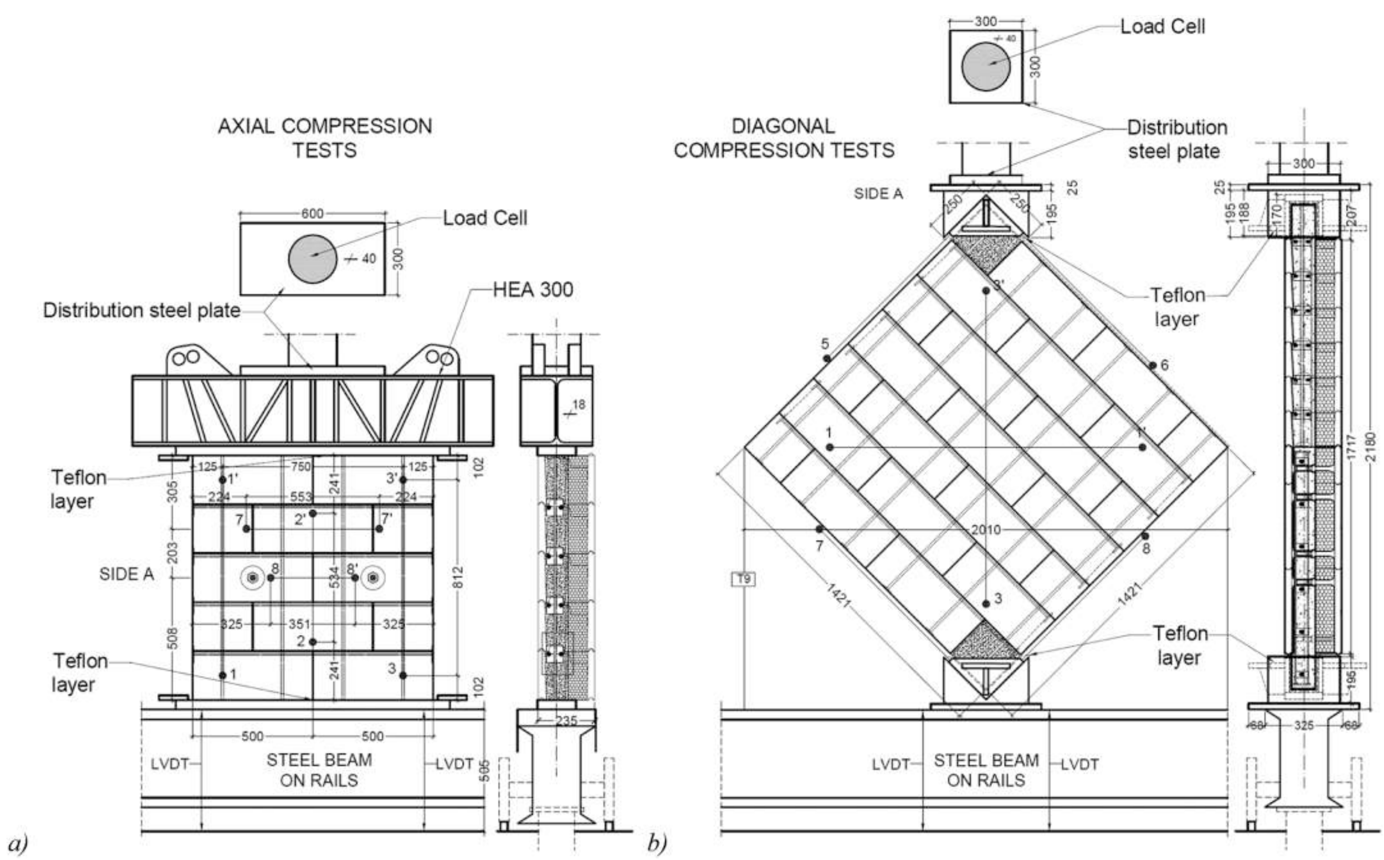


**Fig. 4.** Test setup and instrumentation for a) compression and b) diagonal compression tests.

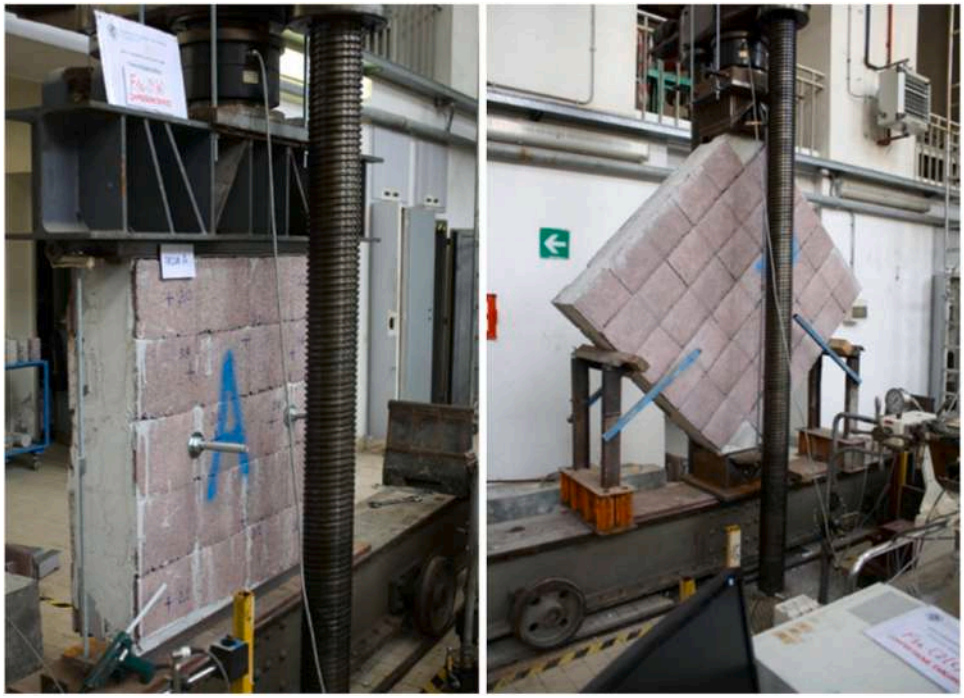

**Fig. 5.** a) axial compression tests, b) diagonal compression tests, c) buckling tests.

load, whose values was estimated through preliminary numerical simulations; each loading step was kept constant for about one minute to measure the deformations. The load was finally increased until failure with a testing rate of 4 kN/sec.

For the execution of diagonal compression tests, the specimens were placed in the machine rotated by 45° respect to the loading direction. The load was applied in correspondence of the corner, preventing local failures thanks to the adoption of the rigid steel corners for load redistribution. LVDT were positioned along the two diagonals on the two sides of the specimens; additional ones were used to measure the vertical displacement of the bottom steel beam for load application. The tests were performed monotonically increasing the load till failure, with a testing rate of about 1.0 kN/sec.

### 3.1.3. Experimental tests' results

According to [23], compression and diagonal compression tests were devoted to determine the ratio between secant stiffness corresponding to maximum load and secant stiffness corresponding to the 30% of the maximum load. For compression axial load tests, the expected failure load – according to numerical simulations performed – was 1952 kN; the values achieved during the tests were respectively equal to 1412 and 1846 kN. In the first sample, the reduced load was related to the unperfect realization of the concrete cast leading to the concentration of stresses mainly in correspondence of one side of the concrete wall and to the premature failure of the sample. The ratio $K(F_{\max})/K(0.3F_{\max})$, whose evaluation is prescribed according to [23], resulted equal to 2.23 and 1.38 respectively for the first and the second sample, the first value reflecting the unperfect casting.

In case of diagonal compression loads, the expected failure load, once again according to numerical simulations, was 480 kN, against the values achieved during the tests, equal to 466 kN and 401.2 kN. Several adjustments were required during the first test: the unperfect realization of the specimen leaded to the premature cracking in correspondence of the corner where the load was applied and to the onset of local buckling phenomena. The specimen was therefore unloaded and then reloaded after the adoption of specific precautions to achieve the global failure of the sample. The numerical predictions, performed considering the equivalent continuous RC wall with equivalent thickness defined according to (1) were almost reliable in estimating the structural performance of the system if the concrete cast is adequately compacted and if defects are avoided.

This preliminary tests, despite the limited relevance in the overall scenario, evidenced the need of the accurate realization of the concrete cast since strongly influencing the tests' results ( Table 4).

## 3.2. Out of plane tests for buckling performance

### 3.2.1. Design of the specimens

Specimens were designed to be representative of slender panels in existing buildings; resulting dimensions were equal to 150 cm × 285 cm x 23.5 cm ($L/H$ ratio about 1:2). The specimens consisted of 14 rows of formwork blocks organized as presented in Fig. 6a; where needed, blocks' dimensions were adapted through circular saw cutting. Concrete class C25/30 (S4) and rebars B450C were used; the nominal thickness of the concrete layer was equal to 100 mm. Vertical (ϕ10/25) and horizontal (2ϕ6/20) rebars were adopted; steel plates (70×70×6 mm and 40×50×6 mm, respectively) were introduced to fix the rebars at the two ends for avoiding slippage during the test and to provide adequate support during the assembly.

In correspondence of the first and of the last rows, the formwork ribs were removed to provide continuity to the concrete cast. RC beams were introduced in correspondence of the top and of the bottom sections of the specimen allowing the connection to the testing machine. The concrete cast was realized in two steps, providing continuity to reinforcements and an efficient compacting despite the reduced thickness of the concrete layer.

### 3.2.2. Test setup

Tests were performed using a universal compression machine Mohr & Federhaff with 3000 kN of capacity. A preliminary check of the correct realization of the specimens (verticality, effective thickness of the concrete layer, etc.) was performed, since strongly influencing results as proved by previous tests. Due to the shape of the formwork blocks and to the position of the insulation layer, the concrete cast was not centered with respect to the blocks: supporting components were then introduced to ensure the axial load be applied only on the concrete layer. A rigid

**Table 4**
Summary of results achieved from axial compression and diagonal compression tests.

| Compression tests | | $F_{max}$ | 30% $F_{max}$ | $\delta_{max}$ | $\delta_{0.30}$ | $K_{max}$ | $K_{0.30}$ | $A_{eq}$ | σ |
|---|---|---|---|---|---|---|---|---|---|
| | | [kN] | [kN] | [mm] | [mm] | [N/mm] | [N/mm] | [mm$^2$] | [MPa] |
| Axial | n.1 | 1411.2 | 470.4 | 15.5 | 11.5 | 91308 | 41064 | 82890 | 17.02 |
| | n.2 | 1845.7 | 615.2 | 7.4 | 3.4 | 248053 | 179223 | 82890 | 22.27 |
| Diagonal | n.1 | 466.0 | 139.8 | 21.8 | 7.2 | 21376 | 19417 | - | - |
| | n.2 | 405.9 | 121.8 | 18.8 | 8.7 | 21590 | 14064 | - | - |

steel beam was used to transfer the axial load to the specimen: the load was then uniformly redistributed on the surface achieving uniform displacements in correspondence of the loaded areas. Steel plates and levelling Teflon layers were also placed at the top and bottom of the specimen.

An increasing monotonic load was applied until failure (i.e. when a 20% load decrease is achieved) with testing rate equal to 3.0 kN/sec. Load acquisition was performed continuously through a 3000 kN capacity load cell; to measure the of the out-of-plane displacements, core LVDT transducers (length range equal to 0÷200 mm and 0÷100 mm) were used, respectively in correspondence of H/4, H/2 and H/6. Spring transducers were placed in correspondence of the bottom steel beam (Fig. 6b). Temporary steel structures were designed to support the technicians during testing operations, to allow the placing of the instrumentations and to measure and monitor the out-of-plane displacements.

### 3.2.3. *Experimental tests' results*

The failure mechanism involved the three upper blocks' rows of the specimens, for about the whole specimen's length from the right side (Fig. 7b-d). The out-of-plane buckling mechanism, mainly located in correspondence of half of the height, was associated to the development of an inclined failure surface. The horizontal failure plane generated on the left side of the sample (Fig. 7b) was, on the other hand, traced back to the instant immediately following the failure due to buckling, i.e. the rotation of the upper base of the specimen following the lack of support on the opposite side. Thanks to the top and bottom RC beams, simulating the effective conditions of the retrofit panel in existing buildings (i.e. a double restrained wall) leaded to values of the load activating buckling up to 2655 kN, higher respect to what achieved from simulations. It can be therefore concluded that no buckling issues are expected for the design nominal thickness 100 mm.

## 3.3. *Tests for horizontal monotonic and cyclic loads*

### 3.3.1. *Design of the specimens*

Specimens for horizontal monotonic and cyclic tests were realized with different geometries, with $L/H$ ratios (about) 1:2, 1:1 and 4:3 (Fig. 8). Considering the dimension of the formwork blocks, the resulting height of the panel (excluding the RC top beam) was 284 cm; the lengths were, respectively, equal to 150, 300 and 400 cm. Each specimen was provided by a proper foundation system and by a RC top beam of dimensions, for all $L/H$, equal to 60 × 30 cm and 20 × 25 cm.

The typical reinforcement layout of the panels consisted in horizontal rebars 2ϕ6/20 connected at the ends to steel plates of dimensions 70×70×6 mm and vertical reinforcements ϕ10/25 continuous till the top RC beam, where an opportune anchorage was realized. Hook rebars ϕ10/25, overlapping the vertical bars for about 70 cm, were used for the connection with the foundation. This latter presented longitudinal bars ϕ16 and stirrups ϕ10/10 cm (middle section) and ϕ10/5 cm (end sections). Before casting, holes were realized in the foundation to allow the connection to the laboratory strong floor. The top RC beam, centred with the RC layer, showed longitudinal bars 3ϕ16 (top and bottom) and stirrups ϕ8/25; holes were realized in the concrete casting (spaced by 375 mm) for the connection to the loading system.

Concrete class C25/30 was used, with slight variations in the different castings and values of the cylindric concrete strength of the walls ($f_{cm}$) varying between 25.6 and 31.3 MPa. Higher average values were achieved for the foundation (36.9 MPa) and for the RC top beam (48.9 MPa). B450C rebars with yielding ($f_y$) and tensile ($f_u$) strength respectively equal to 508 and 597 MPa (specimen 4:3) and 533 and 614 MPa (specimens 1:1 and 1:2) were used, with $A_{gt}$ values around 9%.

### 3.3.2. *Test setup and instrumentation*

One horizontal monotonic and two cyclic tests were performed for each geometrical configuration. The setup and instrumentation were the same for all the different $L/H$ ratios (with necessary adaptations), speeding up the assembly and de-assembly procedures. Panels were subjected to a vertical load simulating the weight of an upper panel of similar dimensions, in case of application to two-storeys buildings (the retrofit system is conceived not to carry on vertical loads coming from horizontal storeys). Horizontal displacements were applied in a quasi-static way, avoiding relevant dynamic effects, using hydraulic jacks anchored to the steel contrast frame of the laboratory of Pisa University. The uniform redistribution of the load, applied in correspondence of the top RC beam, was guaranteed by a rigid steel transverse beam (Fig. 10).

The whole test setup therefore consisted in: *(a)* the vertical load application system, *(b)* the horizontal displacement/load transfer system, *(c)* the supporting steel structures avoiding out-of-plane mechanisms, simplifying the assembly operations and allowing to control the test's execution.

The vertical load was introduced through 4 Dywidag rebars ϕ27 connected to the contrast base frame; the application system was symmetric with respect to the axis of the RC layer and the load was kept constant for the whole test's duration. Two hydraulic jacks (Enerpac RC 108, stroke ± 203 mm, load capacity 101 kN), located between two HEB200 (one top, one bottom) providing the correct load redistribution on the panel, were introduced (Fig. 10).

The horizontal displacements were applied through two hydraulic jacks (stroke ± 250 mm, load capacity 400 kN) connected, from one side, to the steel contrast wall of the laboratory and, from the other side, to the rigid steel transverse beam allowing the load application in correspondence of the top RC beam of the retrofit panel. The rigid transverse beam, made up of HEM160 and similar profiles (Fig. 11), was connected to the retrofit panel through 2UPN140 located on the two opposite sides of the RC top beam. The connection between the UPN and the rigid transfer beam was realized through 4M4 class 8.8 spaced by 375 mm. To join the UPN profiles to the RC beam, passing M27 were introduced in holes prepared before casting and fixed through chemical injection grouting.

The connection to the laboratory strong floor was realized through the RC foundation system, adequately rigid not to overcome deformations affecting both the test's execution and the results' interpretation. Two different steel frames were realized for the connection laboratory/foundation: a steel top frame made up of HEB400 used to fix the sample allowing the correct behaviour of the shear contrasts and a bottom frame realized with composite UPN200 beams and overhanging IPE360, allowing the anchorage of the sample through M27 rebars (Fig. 11).

Two supporting steel braced frames were, finally, introduced to prevent out-of-plane mechanisms during the tests, forcing the specimen to move only in-plane.

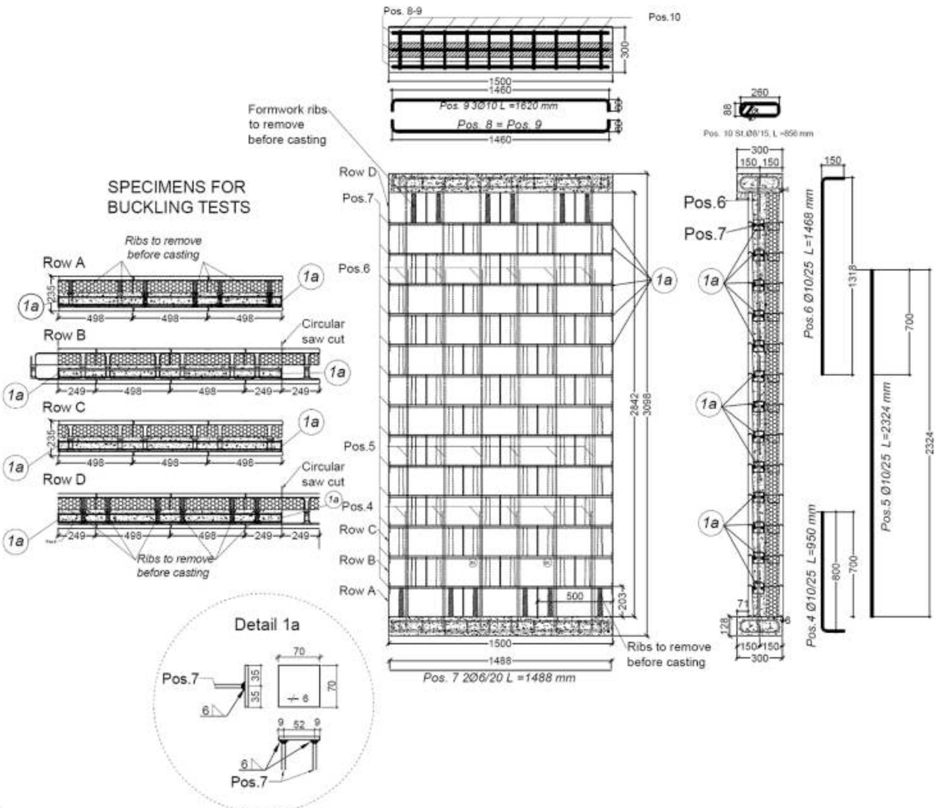


a)

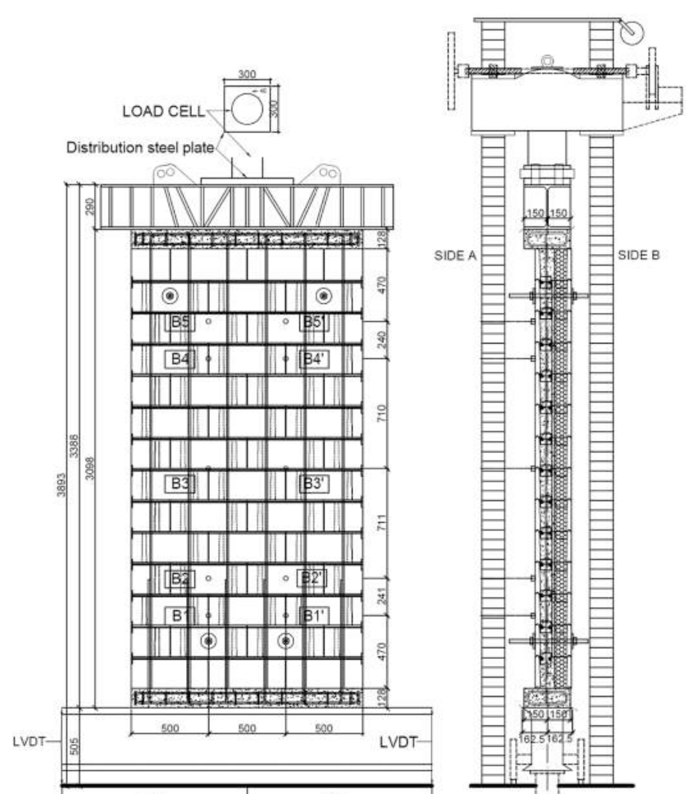


b)

**Fig. 6.** a) Specimen for buckling test; b) test setup and instrumentation.

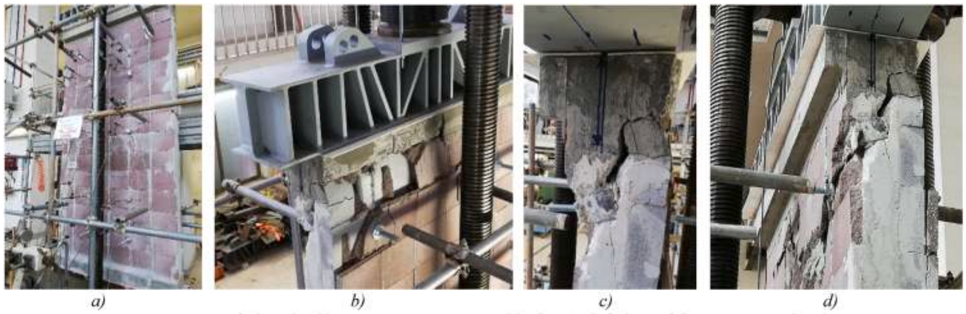


**Fig. 7.** Out-of-plane buckling tests: a) test's assembly, b), c), d) failure of the specimens, details.

The instrumentation layout was designed to measure and control the load entity and the deformation trend during the test. Vertical, horizontal and diagonal transducers, load cells and inclinometers were used. Load cells were located in correspondence of each hydraulic jack; in-plane displacements at the top, bottom and middle height of the specimen were monitored through LVDT transducers with adequate measuring length (Fig. 11). Relative slip between the laboratory strong floor and the steel frames of the basement, due to possible adjustments of the shear contrasts during the loading phase, were checked. Diagonal deformations and vertical deformations between the retrofit panel and the foundation and between the retrofit panel and the top RC beam were also measured.

Fig. 9 shows several images of the specimens during the assembly phase on the strong floor of the laboratory of Pisa University.

### 3.3.3. Tests' execution and results

The vertical load was applied before the displacement history to represent the effective condition of existing buildings, and kept constant for the whole duration for all the tests. The axial loads applied at the top of the specimens, estimated according to preliminary numerical simulations, were respectively equal to 22.64 kN, 42.73 kN and 59.93 kN for $L/H$ ratio equal to (1:2), (1:1) and (4:3).

According to the indications provided by [23], the load (or displacement) increments should allow the evaluation of the elastic stiffness of the panel and the modification of the performance due to cracking (for bending and/or shear forces), the yielding of the rebars and other possible degradation effects, e.g. concrete crushing, rebars' buckling, sliding between foundation and panel, rupture of the rebars, etc.

Monotonic tests were performed till the achievement of a relevant failure mode. Fig. 12 shows the results of the monotonic tests for the different $L/H$ ratio; the corresponding maximum values of horizontal load and top displacement (purified by small displacements in correspondence of the foundation system, measured through the ad-hoc transducers) are summarized in Table 5. Absolute values of the horizontal displacements are presented. As visible, differences around 30% were achieved for specimens (1:1) and (4:3); specimen (1:2) highlighted a lower stiffness, corresponding to higher displacements.

For all the $L/H$ ratio specimens, damages were concentrated at the connection between the foundation system and the panel, leaving the rest of the panel almost undamaged. As visible from Fig. 13, severe cracks were observed in correspondence of the base section under positive bending action (right side of the specimen), in relation to the load application direction. The sudden drops of the load, visible from Fig. 12, were associated to the rupture of the rebars in correspondence of the connection surface between the RC foundation system and the specimen, and to the following cracking of the formwork block (Fig. 13).

Cyclic tests were performed according to the lateral load displacement history presented in Fig. 14a; for each displacement increment, three cycles were performed according to the general protocol proposed by ECCS45 [30] procedure and considering the displacement yielding value as derived by the monotonic performance. For each geometrical configuration, two cyclic tests were performed.

The results of the experimental cyclic tests, in terms of load/drift diagrams, are presented in Fig. 14(b), (c) and (d) respectively for specimens (1:1), (4:3) and (1:2). The drift was evaluated with reference to the sum of the panels' height (284 cm) plus half of the RC top beam height. The behaviour was almost symmetric (Table 6), as expected considering the reinforcement layout.

In case of specimens (1:1) (Fig. 14b), despite the symmetry of achieved loads, one sample (test #2) showed lower values of the horizontal capacity, with maximum values respectively equal to − 230 kN and + 226 kN against ± 270 kN of the other specimen (test #1) and of what observed during the monotonic test. This variation, even if not so relevant, may be related to the unperfect realization of the concrete cast inside the formwork blocks and to the related material properties.

In case of specimens (4:3) (Fig. 14c), one test (test #2) highlighted a strong asymmetric performance, with maximum loads respectively equal to − 457 kN (→) and + 395 kN (←); in the other case, the behaviour was symmetric but with values of the maximum horizontal load (about ± 400 kN) lower than the one highlighted during the monotonic test. The asymmetry of the cyclic performance was probably caused by the unperfect realization of the specimen, and this is related to the concrete casting and to the possible shift of rebars. These last considerations can be made also for specimens (1:2); as visible from Fig. 14d, in case of test 2 the cyclic performance is highly asymmetric, with achieved load values equal to − 75.6 kN (→) and + 91.3 kN (←).

Similarly to what observed during the monotonic tests, for all the different configurations, the main issues were related to damages in correspondence of the connection between the foundation system and the different specimens (Fig. 15), with sudden failures of longitudinal rebars (ϕ10) in tension in the right or left side of the base section in relation to the direction of the horizontal load. Rebars failures are well recognizable in the diagrams, since related to the sudden decrease of the load. The typical pinching effects of RC wall systems under horizontal loading conditions was strongly recognizable in all the specimens.

## 4. Numerical modelling and calibration

Numerical modelling and simulations of the retrofit panel were performed; results were used to check the reliability of design assumptions and to perform additional investigations about the structural behaviour, the dissipative capacity, the influence of rebars layout etc. The current scientific literature provides different modelling approaches for simulating and analysing RC walls, in relation to the geometric properties, to the relevant performance (flexural/ductile, shear/brittle) and to the modelling level (i.e. single wall, whole building, etc.). Takayanagi and Schnobrich [31] proposed a block model for the RC wall, where the single panel was divided into a defined number of blocks modelled through a rotational nonlinear spring in the middle section, accounting for axial force/bending interaction. Mono-dimensional models to represent bi-dimensional panels were often adopted in the

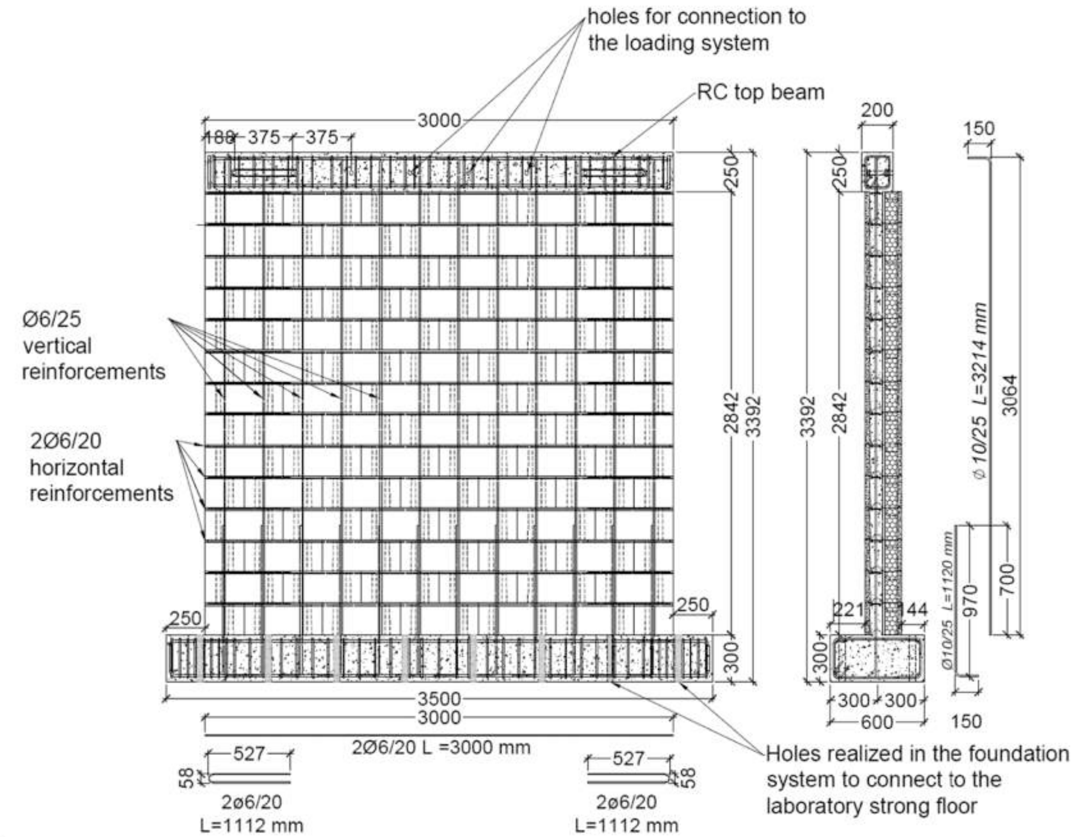


a)

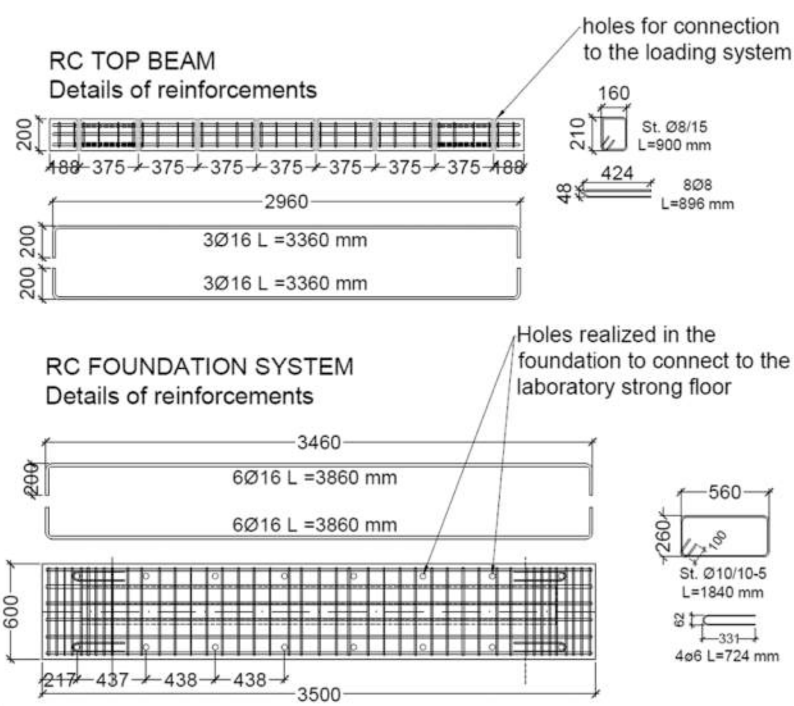


b)

**Fig. 8.** Specimen for horizontal tests (L/H ratio equal to 1:1): a) overall view and b) details of reinforcements and realization of RC top beam and foundation system.

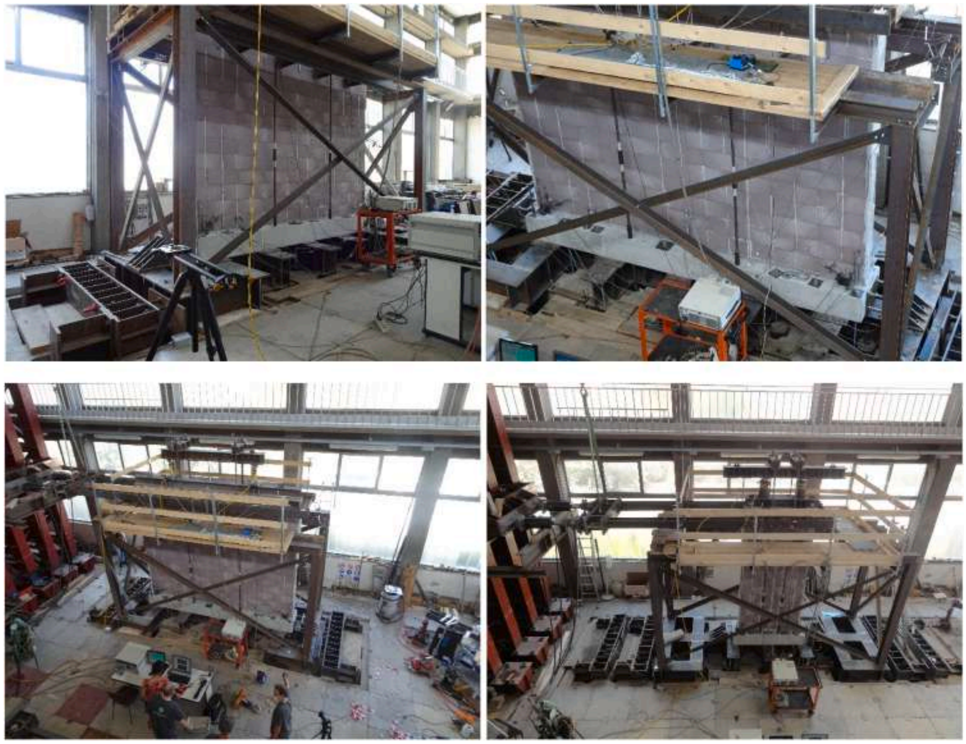

**Fig. 9.** Assembly of the specimen setup on the strong floor of the laboratory of Pisa University (different L/H ratio specimens).

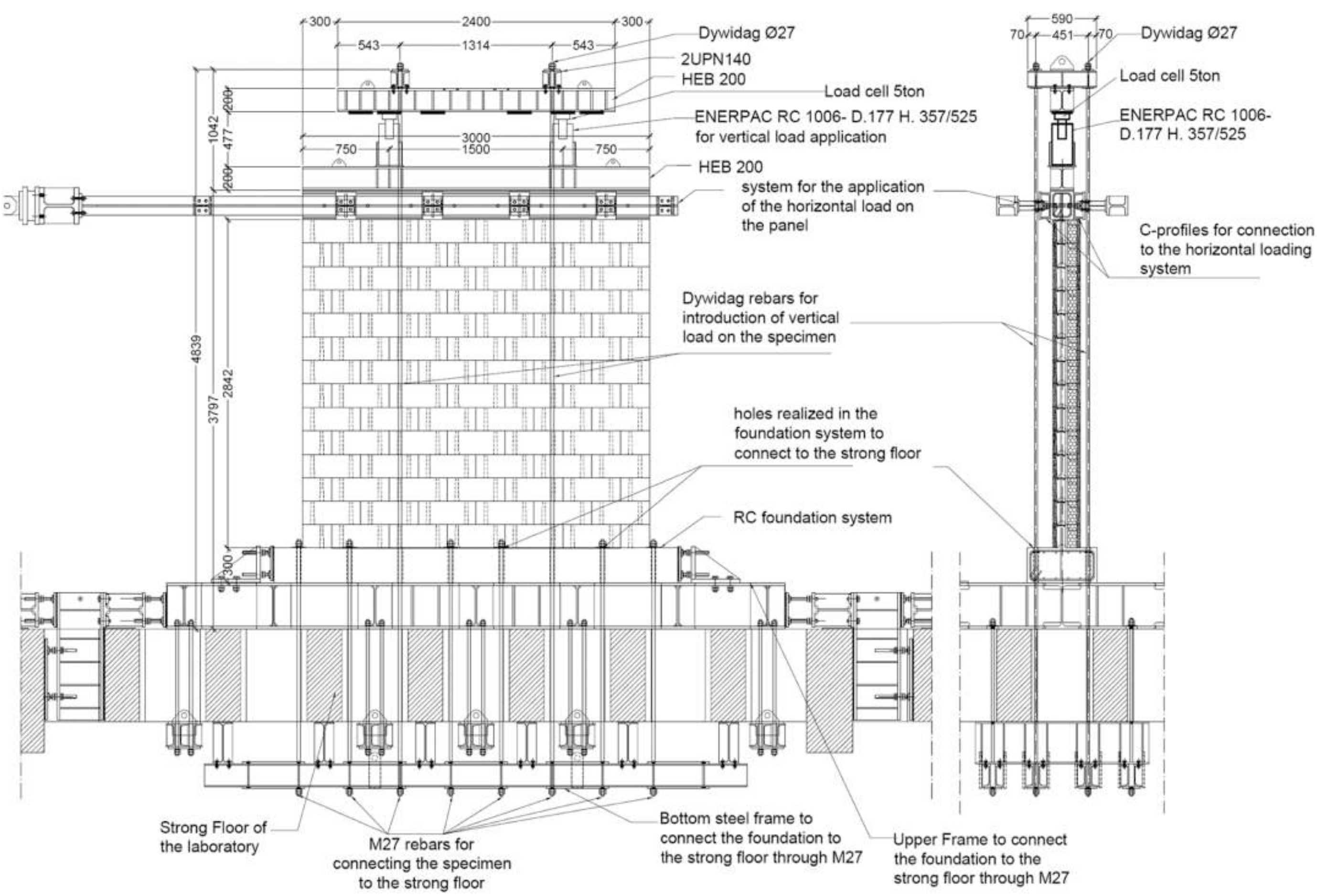


**Fig. 10.** Test setup, specimen with L/H ratio (1:1).

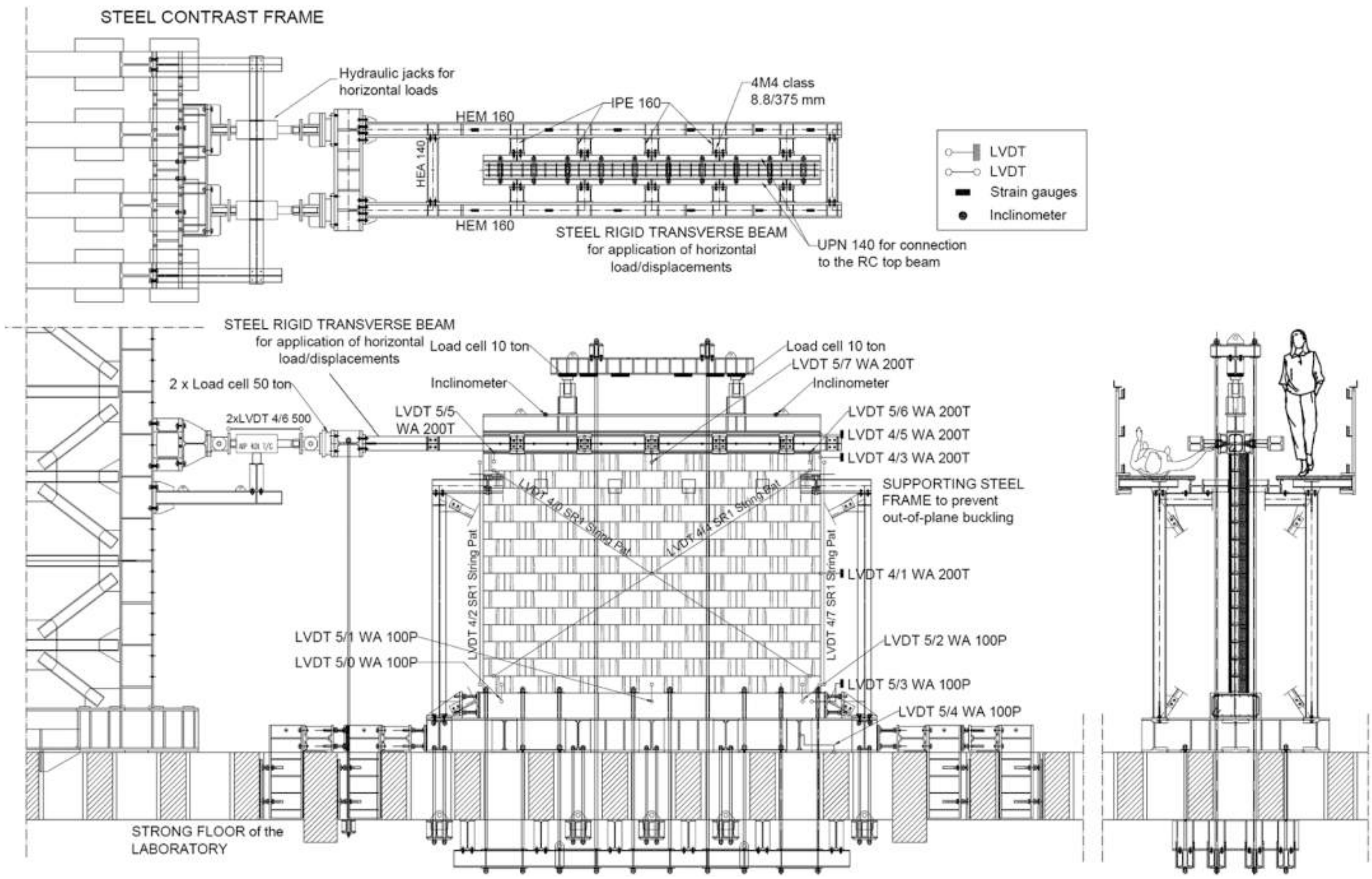


**Fig. 11.** Overall test setup with connection to the strong floor and the strong wall of the laboratory, supporting steel structures and localization of test instrumentation (specimen with L/H ratio 4:3).

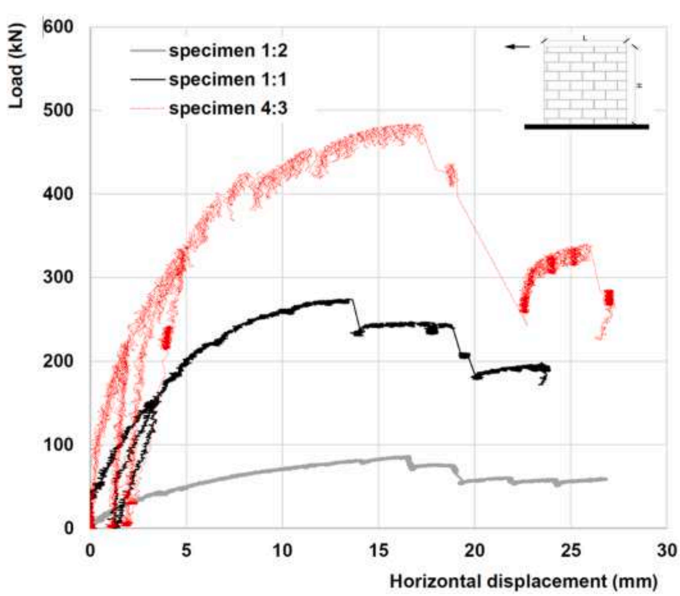


**Fig. 12.** Monotonic horizontal load/displacement diagrams for the three different specimens.

past thanks to the reduced computational effort, despite the strong simplification introduced. Orakcal et al. [32] proposed a macro-fibre model made up of a linear central elastic element with nonlinear axial and rotational springs at the ends. The connection with other components was realized through rigid end zones; opportune constitutive laws

**Table 5**
Summary of monotonic horizontal tests on specimens.

| L/H specimen | $F_{max}$ | $d_{max}$ | d ($F_{max}$) | $F_{max}$ /$d(F_{max})$ |
|---|---|---|---|---|
| | [kN] | [mm] | [mm] | [N/mm] |
| 1:2 | 86.73 | 27.26 | 16.59 | 5227.8 |
| 1:1 | 274.4 | 23.94 | 13.35 | 20556.1 |
| 4:3 | 484.1 | 27.32 | 16.90 | 28646.1 |

for springs, representing the performance of the panel, allowed to account for stiffness variation in relation to the acting loads. Further developments were proposed: for instance, the MVLEM (Multiple Vertical Line Element Model) coupled several macro-fibre models with the aim of correctly representing the flexural performance, introducing two rigid beams in correspondence of the top and bottom levels. The model proposed by Fishinger et al. [33] optimized the described MVLE model introducing a horizontal spring representing the bending/shear interaction. Panagiotou et al. [34] proposed a nonlinear truss model to describe the cyclic performance of RC panels, comparing the combined axial/bending/shear behaviour of a generic RC wall under in-plane actions to a nonlinear strut-and-tie model. Experimental tests were used for calibration; a good representation of the post-cracking behaviour, the peak horizontal capacity, the deformation performance, etc. was achieved.

In the present work, a simplified mono-dimensional model was proposed for the retrofit panel; despite all the above-mentioned limits, it proved to be a reliable preliminary tool for representing the structural performance of the proposed system.

**Fig. 13.** Tests' execution and damages in correspondence of the connection between the foundation system and the sample.

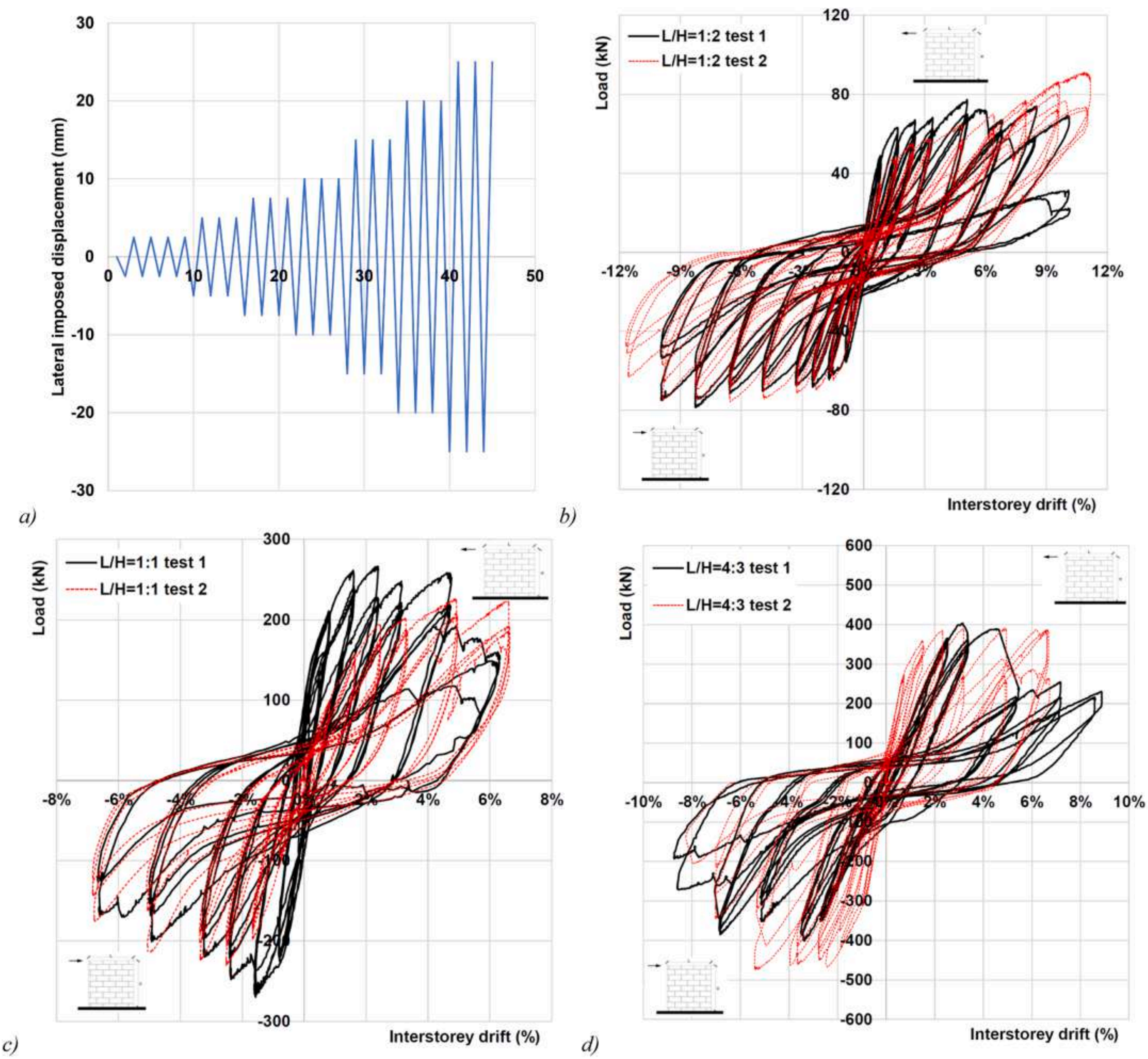


**Fig. 14.** Cyclic test: a) displacement history; load/displacement behaviour of specimens a)1:2, b) 1:1 and c) 4:3.

### *4.1. Model description and calibration*

A simplified mono-dimensional nonlinear model was elaborated to represent the structural monotonic and cyclic performance of the retrofit panel; the only concrete layer with equivalent thickness ($t_{eq}$) defined by Eq. (1), neglecting the contribution provided by the formwork blocks, was considered. The model was realized using OpenSees® [35]. A 'nonlinearBeamColumn' element was used to represent the RC wall, whose transversal section was defined according to the effective length of the considered panel in relation to the different *L/H* geometry, being

**Table 6**
Summary of results coming from experimental cyclic tests (load and displacements).

| *Specimen (L/H)* | *Test #* | *Load direction* | *$F_{max}$ [kN]* | *Disp $_{max}$ [mm]* | *drift* |
|---|---|---|---|---|---|
| ***1:2*** | Test 1 | → | -78.56 | -29.56 | -10.0% |
| | (07.07.2022) | ← | 77.37 | + 30.07 | 10.1% |
| | Test 2 | → | -75.64 | -34.68 | -11.7% |
| | (21.07.2022) | ← | 91.34 | + 33.09 | 11.2% |
| ***1:1*** | Test 1 | → | -269.54 | -19.82 | -6.7% |
| | (22.03.2022) | ← | 266.51 | + 18.75 | 6.3% |
| | Test 2 | → | -230.70 | -20.29 | -6.8% |
| | (27.04.2022) | ← | 226.71 | + 19.69 | 6.6% |
| ***4:3*** | Test 1 | → | -401.13 | -25.93 | -8.7% |
| | (03.02.2022) | ← | 403.35 | + 26.33 | 8.9% |
| | Test 2 | → | -475.18 | -24.47 | -8.3% |
| | (13.06.2022) | ← | 391.74 | + 19.95 | 6.7% |

the effective height (*H*) of the panel (and of the monodimensional element) equal to 284 cm, and modelled as a fibre section (Fig. 16). The horizontal reinforcements (ϕ6/25) were not introduced in the model, being not adequately anchored and therefore not able to provide a sufficient confinement contribution. The position of vertical rebars in the model slightly differ from the effective one, as a consequence of the shift from the 'real' system with transversal ribs to the modelled continuous concrete wall. The RC section was modelled as symmetric in terms of rebars disposition as in the effective system.

The panel was considered fully restrained in correspondence of the bottom section, thanks to the presence of the foundation system; the RC top beam (reproducing the RC curb of horizontal storeys) was modelled, again, through a 'nonlinearBeamColumn' with adequate section (23.5 ×30 cm).

For concrete, the 'uniaxialMaterialConcrete04′ model was used, able to reproduce the stress-strain compression performance proposed by Popovics [36] until concrete crushing; for the unloading and reloading performance, the Karsan-Jirsa [37] law was adopted. Concrete tensile strength was neglected.

The values of $f_c$, $E$, $G$ and initial stiffness as well as concrete deformations ($\varepsilon_{c2}$ and $\varepsilon_{cu}$) were calibrated basing on experimental tests on materials. For steel rebars, the 'Multilinear Material' model was used for the monotonic behaviour while for the cyclic performance, the hysteretic material law was adopted, whose parameters were calibrated basing on experimental tests' results on rebars B450C. Second order effects were introduced in the model. Fig. 17 shows the result of modelling calibration for the monotonic performance. As visible, the model is able to correctly reproduce the experimental performance, in terms of achieved loads and failure modalities. The achievement of the maximum deformation of rebars corresponds to the sudden drop of the load due to the rebar's failure, as observed during the test; the same can be said for the crushing of the concrete cover, well appreciated during the experimental test (Fig. 15). Slight variation of the stiffness is visible in the elastic range, that do not anyway influence the achievement of load and displacement values as observed during the experimental phase.

The model is also able to correctly reproduce the cyclic behaviour as shown by Fig. 18, for all considered *L/H* configurations.

Exploiting the results of monotonic numerical analyses, the values of the behaviour factors *(q)* were evaluated according to the formulation proposed by Eq. (2) [38]:

$$q = \frac{V_u}{V_y} \bullet \frac{d_u}{d_y} \tag{2}$$

**Fig. 15.** Cyclic tests' execution and details of damage in correspondence of the RC foundation connections (1:2 and 4:3).

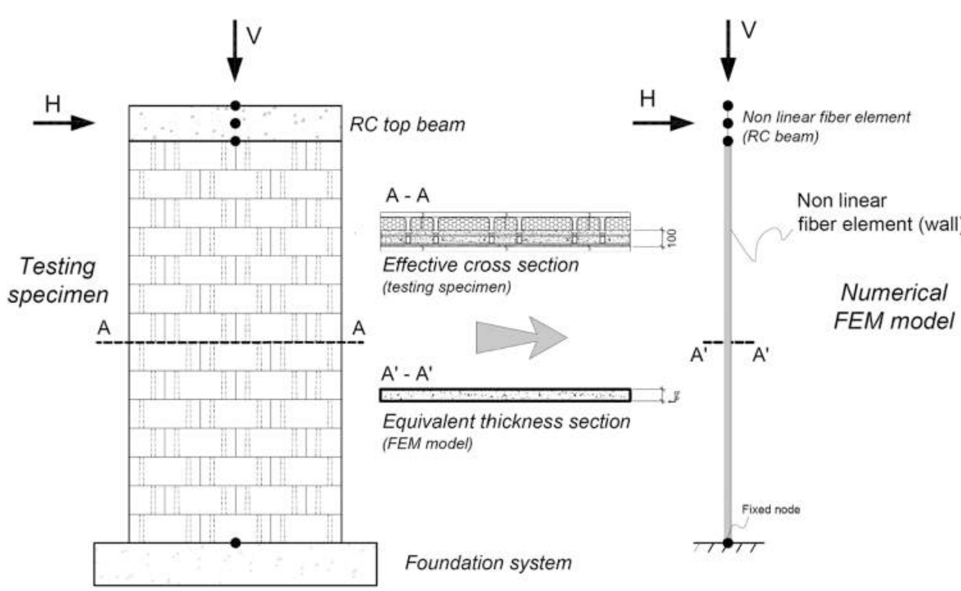


**Fig. 16.** Schematization of slightly RC wall with equivalent thickness, FEM Model.

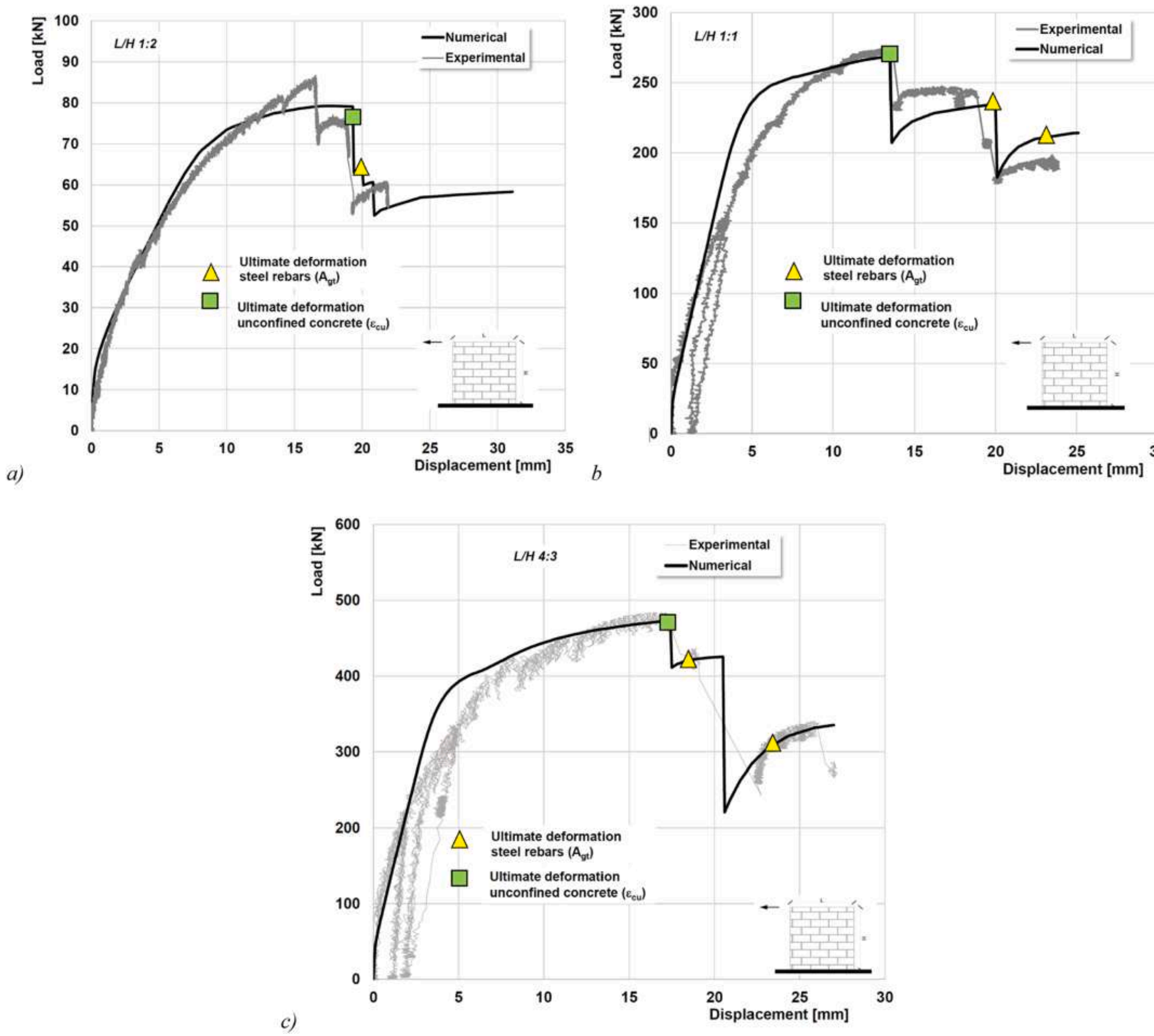


**Fig. 17.** Numerical calibration of the model basing on monotonic experimental tests: L/H a) 1:2, b) 1:1 and c) 4:3.

being $V_u$ and $d_u$ respectively the ultimate base shear and top displacement, $V_y$ and $d_y$ the base shear and displacements corresponding to the yielding. Both ultimate and yielding points were evaluated in correspondence of the achievement of ultimate and yielding chord rotations, whose formulation is provided by the equations C8.7.2.7b and C8.7.2.5 of [26].

Table 7 shows the values of curvatures ($\chi$), plastic hinge length ($L_{pl}$) evaluated according to equation C.8.7.2.6 of [26], chord rotations ($\vartheta$) at ultimate and yielding conditions for specimens with L/H (1:1) and (4:3). Achieved values are aligned with what expected by a slightly reinforced concrete wall designed in medium/low ductility class, with a slightly higher performance in case of specimen (1:2).

### *4.2. Parametric analysis*

A parametric analysis was performed to assess the influence of the variation of relevant parameters on the structural response of the retrofit panel. As known, the tested specimens were characterized by different *L/H* ratios for representing the possible different configurations of the existing masonry buildings, owned the same longitudinal and vertical reinforcements' layout and rebars' diameter (because of both design requirements and practical needs for assembly and standardization during the construction phase) and the same concrete strength class. The variability of the longitudinal reinforcement ratio $\rho_0$ (i.e. 0.4%, 0.5% and 0.7%), however respecting the limits required for RC walls [24,25], and that of the concrete compressive strength (i.e. 20, 30 and 40 MPa) were considered. Note that the variability of the above-mentioned parameters is limited by the restrictions introduced, from one side, by guidelines actually existing for RC systems with formwork blocks [22, 23], and from the other side, by practical requirements related to the reduced dimensions of the blocks themselves. Fig. 19 shows the results of the parametric analyses performed for the different specimens.

The increase of the longitudinal reinforcement ratio caused the increase of the base shear resistance in the retrofit panel: for specimens with *L/H* (1:1) and (4:3) the increase, evaluated respect to the reference condition with $\rho_0$ equal to 0.4%, was respectively around 35% and 70% for $\rho_0$ equal to 0.5%, 0.7%; in case of *L/H* (1:2) the variation was lower, with values up to 25% and 60% respectively for $\rho_0$ equal to 0.5% and

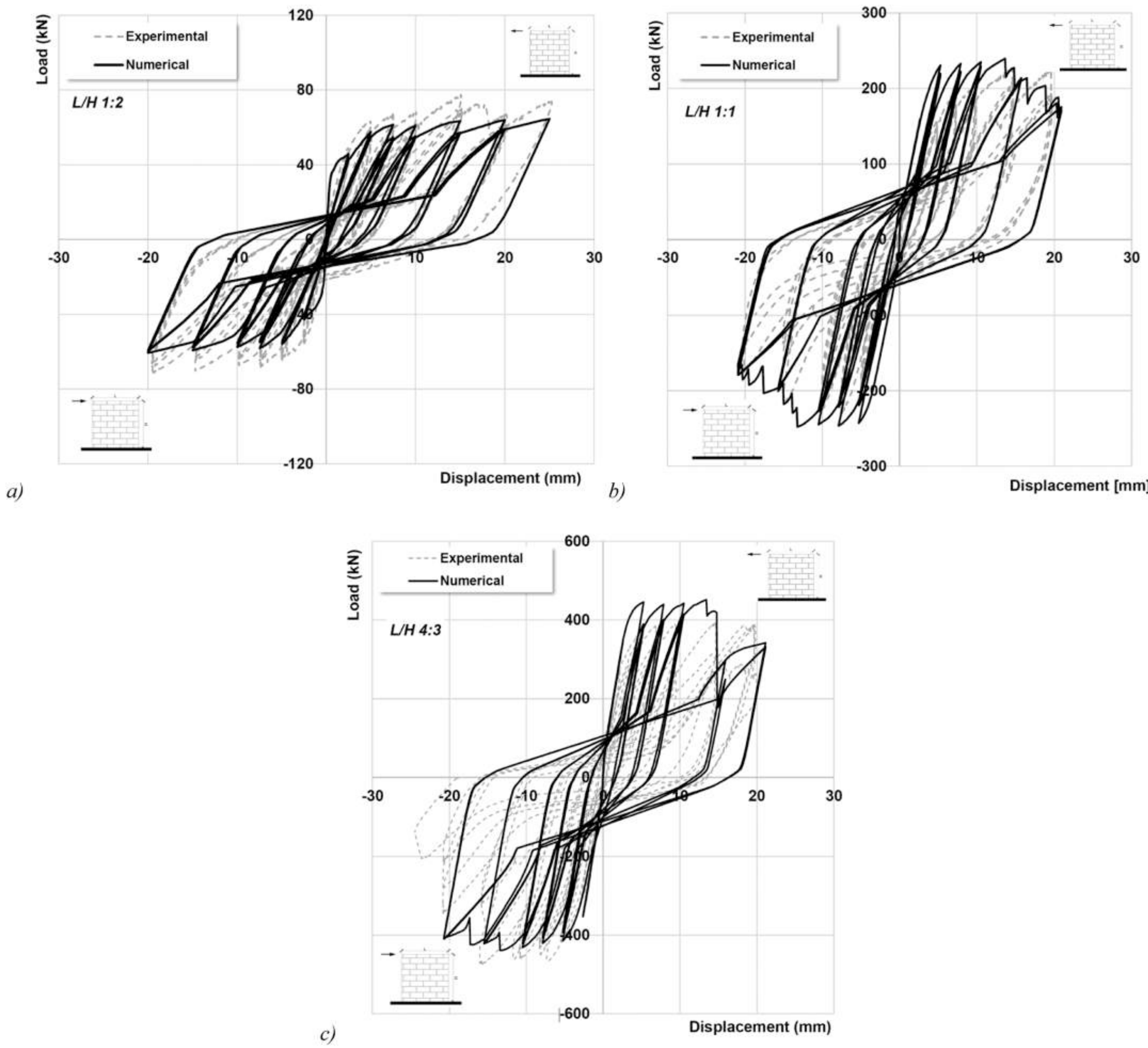


**Fig. 18.** Numerical calibration of the model basing on cyclic experimental tests for specimens a) 1:2; b) 1:1, c) 4:3.

**Table 7**
Achieved behaviour factor and relative evaluation parameters.

| *L/H* | $\chi_y$ (mm$^{-1}$) | $\chi_u$ (mm$^{-1}$) | $L_{pl}$ (mm) | $\vartheta y$ (rad) | $\vartheta u$ (rad) | $d_y$ (mm) | $V_y$ (kN) | $d_u$ (mm) | $V_u$ (kN) | *q* (-) |
|---|---|---|---|---|---|---|---|---|---|---|
| 1:2 | $2.0 * 10^{-6}$ | $2.0 \times 10^{-5}$ | 990 | 0.00641 | 0.0145 | 19.1 | 70 | 41.9 | 75 | 2.31 |
| 1:1 | $9.6 * 10^{-7}$ | $1.05 \times 10^{-5}$ | 990 | 0.00527 | 0.0087 | 15.7 | 226 | 24.9 | 214 | 1.50 |
| 4:3 | $7.5 * 10^{-7}$ | $1.22 \times 10^{-5}$ | 1006 | 0.00506 | 0.0097 | 14.8 | 470 | 29.1 | 355 | 1.49 |

0.7%. Obviously, the base shear increase corresponded to a progressive decrease of the displacement capacity, with lower values of top displacement when the ultimate unconfined concrete or, alternatively, the ultimate steel rebars' deformation was achieved. In any case, the ultimate condition of the retrofit panel was always associated to the rupture of longitudinal bars in tension. Similar considerations can be made concerning the influence of the variation of the concrete strength, where a modest increase of the base shear force associated to higher concrete strength was appreciated, not significantly influencing the structural response of the element.

### 4.3. Preliminary simulations on the retrofitted masonry wall

Preliminary numerical simulations were performed on the retrofitted system (i.e. existing masonry wall + retrofit panel). A nonlinear model of the retrofitted wall was realized using OpenSees® [35]: the model

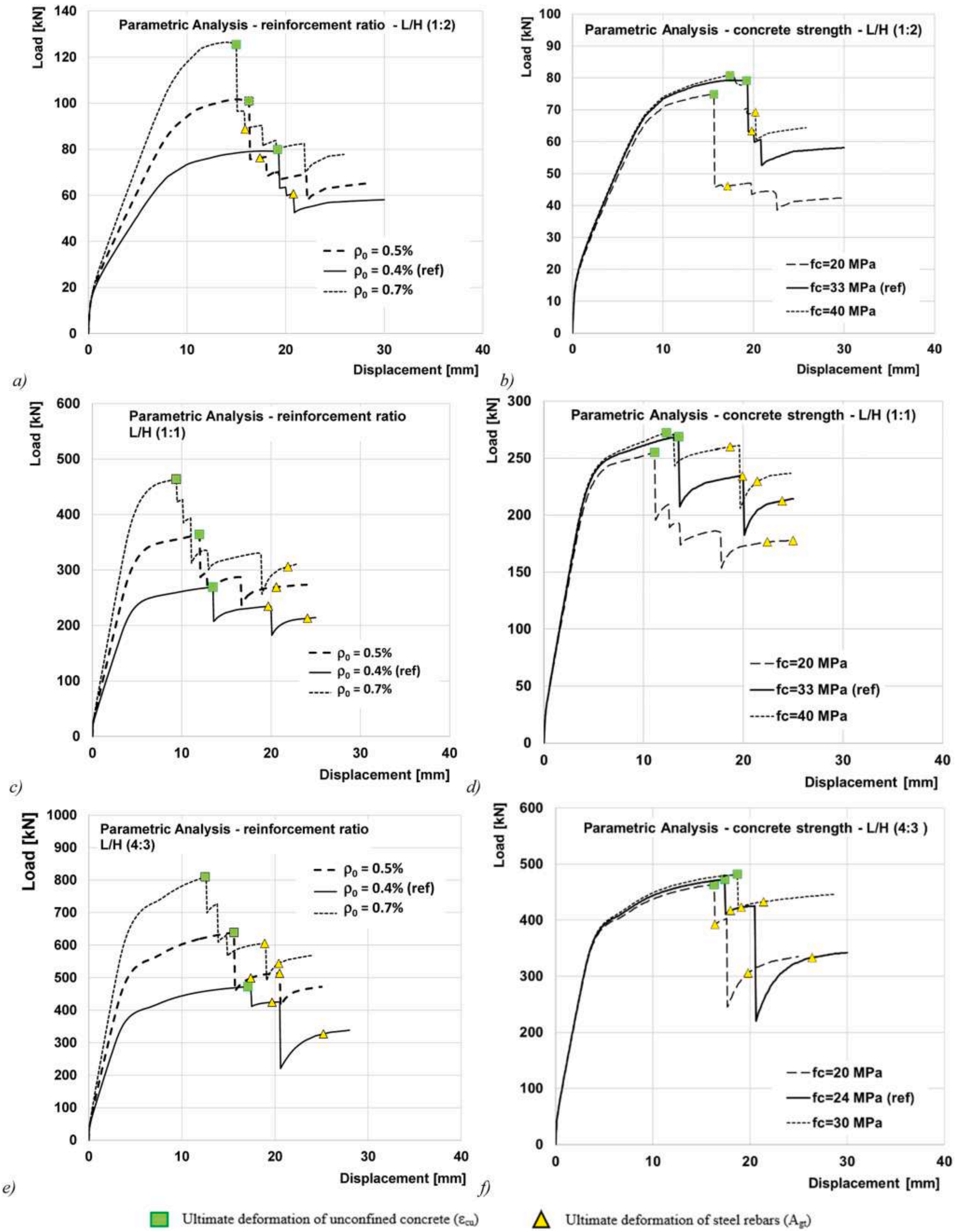


**Fig. 19.** Parametric analysis for: a) L/H (1:2) for reinforcement ratio; b) L/H (1:2) for concrete strength; c) L/H (1:1) for reinforcement ratio; d) L/H (1:1) for concrete strength; e) L/H (4:3) for reinforcement ratio; f) L/H (4:3) for concrete strength.

consisted in two mono-dimensional nonlinear elements used to represent, respectively, the retrofit panel (according to what already presented in the previous paragraph) and the masonry existing wall, with thickness equal to 250 mm (Fig. 20). NonlinearBeamColumn elements with fibre section were used for each panel; two $L/H$ ratios, equal to 1:2 and 1:1 were considered for the simulations. The two elements were considered fully restrained in correspondence of the bottom section, thanks to the presence of the rigid foundation system. At the top of elements, RC curbs were introduced with adequate dimensions. Connections between the two panels, in correspondence of the top level, was realized using rigid link elements able to transfer the only horizontal actions. Vertical loads respectively equal to 148 kN and 22.64 kN (for $L/H$ 1:2) and to 200 kN and 42.75 kN (for $L/H$ 1:1) were applied in correspondence of the masonry wall and on the retrofit panel, accounting for the effective loads acting on a masonry wall extracted from a real building (for example the one presented in chapter 2) and for the weight of a similar retrofit panel, i.e. in presence of a second floor level.

For the masonry wall, the values of mechanical properties were derived from experimental tests performed on DoppioUNI blocks and poor cement mortar (aiming to represent a real existing wall), providing values of compression strength and elastic modulus E respectively equal to 5.90 MPa and 5700 MPa. A limited the tensile strength was also introduced. For the equivalent thickness concrete panel ($t_{eq}$ equal to 82.89 mm) the same modelling assumptions already presented in §4.1 were adopted.

Fig. 21 shows the results in terms of load – displacements curves of the coupled system in the two different $L/H$ configurations (1:2) and (1:1) achieved from a simple nonlinear pushover analysis with increasing horizontal action. In the figures, the pushover curves are presented for the coupled system, the single masonry wall and the retrofit panel. Load-displacement curves were stopped in correspondence of the achievement of a relevant collapse criterion, i.e. the reaching of the ultimate rotation in case of the retrofit panel and in the coupled system (being its performance under seismic action governed by the RC wall introduced) and the trigger of the first relevant collapse modality (shear or bending) for the masonry panel. A strong improvement of the structural performance of the existing masonry wall can be appreciated, with the maximum horizontal load sustained shifting from 35 kN to 118 kN (for the 1:2 $L/H$ configuration) and from 95 kN to 360 kN (for the 1:1 $L/H$ configuration), highliting how the resulting performance of the retrofitted system is governed by the proposed retrofit panel one, in terms of both forces and displacements.

## 5. Conclusions

A new solution for the combined seismic and energy retrofit of existing masonry buildings, realized through the application of lightly RC walls made by expanded-clay formwork blocks is presented and deeply analysed both numerically and experimentally. The proposed system is aligned with the European Commission's goals, whose interest in improving the seismic performance and reducing the energy consumptions together is progressively growing up. The geometry of the blocks allows the realization of a RC layer (with nominal thickness 100 mm), reinforced both vertically and horizontally, together with the introduction of an insulation panel. The system is conceived to work in parallel with the existing building: the panels are connected to the masonry walls only in correspondence of the horizontal storeys through opportune steel anchorages, carrying on the horizontal actions while the vertical loads weight upon the existing masonry walls, becoming therefore secondary elements. The conceptual design and its optimization through the application to an existing residential case-study building are presented, showing the ability of the proposed system of satisfying the safety requirements imposed by current standards, improving the bearing performance against shear, in-plane and out-of-plane bending actions. Preliminary indications about design, reinforcement layout, connection to foundation and to the existing structure are provided. The typical reinforcing layout consists in a double layer of horizontal reinforcements together with a single layer of vertical rebars, leaving meanwhile the possibility of being increased if necessary, compatibly with the blocks' geometry and the reduced thickness of the concrete casting.

Experimental in-plane and out-of-plane tests on the proposed standalone retrofit panel have been performed: they represent the first step of a wider research project aiming at investigating the effects of the proposed system when applied to existing masonry buildings. Besides, experimental tests allow to assess the reliability of actual indications for the design of lightly RC walls in formwork blocks. Results evidenced a typical failure modality with the breaking of the vertical rebars in

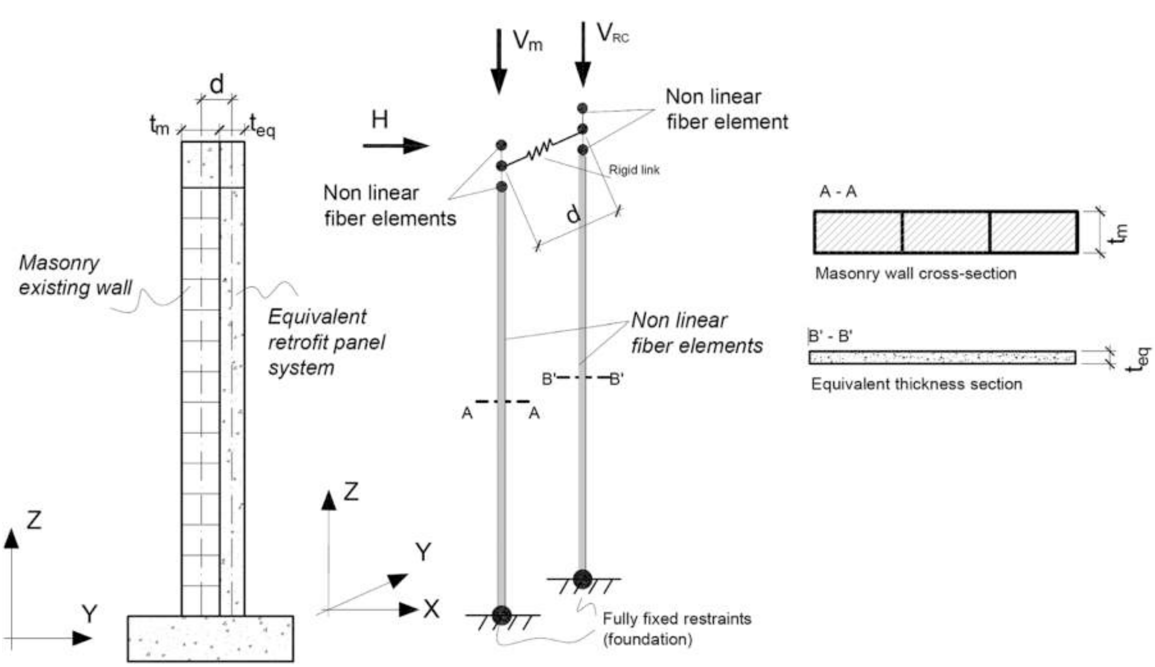


**Fig. 20.** Schematization the preliminary model representing the coupled system existing masonry wall + retrofit panel.

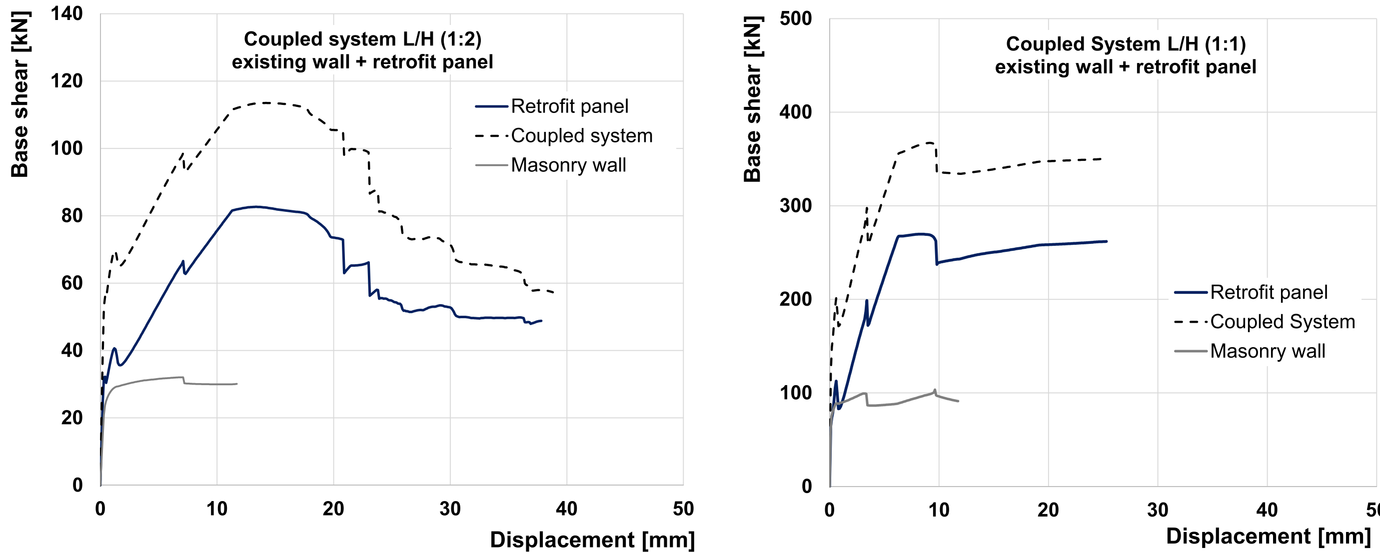


*(a)* *(b)*

**Fig. 21.** Results of numerical nonlinear analysis of coupled system: a) L/H= 1:2, b) L/H= 1:1.

correspondence of the connection with the foundation system, denoting a relatively brittle collapse performance as expected from ordinary slightly RC walls due to the reduced amount of longitudinal reinforcement. A simple numerical monodimensional model has been finally elaborated and calibrated basing on experimental results, showing a good capability, besides the strong simplification, in representing the experimental performance. Parametric analyses have been performed with the aim of assessing the influence of relevant parameters (i.e. the reinforcement ratio – in the range foreseen by current standards; the concrete strength class) and of evaluating the possibility of extending the adoption of the proposed system to a wide range of existing situations, even if the effective variations of such entities are practically limited by both current practical indications and by the reduced thickness of the blocks. As a general remark, experimental tests allowed to assess the reliability of current guidelines [22,23] normally adopted for new constructions in lightly reinforced concrete walls with formwork blocks. Further experimental tests are actually ongoing for assessing the performance of the combined retrofit panel + existing walls.

## CRediT authorship contribution statement

**Simonetti Gemma:** Conceptualization, Data curation, Formal analysis, Investigation, Methodology. **Badalassi Massimo:** Conceptualization, Data curation, Formal analysis, Methodology. **Caprili Silvia:** Conceptualization, Data curation, Methodology, Project administration, Supervision, Validation, Writing – original draft, Writing – review & editing. **Salvatore Walter:** Investigation, Conceptualization, Funding acquisition, Project administration, Resources, Writing – review & editing. **Mattei Francesca:** Data curation, Formal analysis, Investigation, Validation, Writing – original draft, Writing – review & editing. **Chellini Giuseppe:** Data curation, Formal analysis, Investigation.

## Declaration of Competing Interest

The authors declare that they have no known competing financial interests or personal relationships that could have appeared to influence the work reported in this paper.

## Data availability

No data was used for the research described in the article.

## Acknowledgements

The present work was developed in the framework of a research grant collaboration funded by PAVER Costruzioni S.p.A. The Authors would like to thank Paver engineers and technicians for their kind collaboration and for the strong effort in realizing the specimens during all the testing phases.

## References

[1] Italiano Annuario Statistico. Istituto nazionale di statistica (ISTAT), Roma, Italy. 2019.
[2] Losanno D, De Domenico D, Madera-Sierra IE. Experimental testing of full-scale fiber reinforced elastomeric isolators (FREIs) in unbounded configuration. Eng Struct 2022;260:114234.
[3] Tomaževic M, Klemenc I, Weiss P. Seismic upgrading of old masonry buildings by seismic isolation and CFRP laminates: a shaking-table study of reduced scale models. Bull Earthq Eng 2009;7:293–321.
[4] Morelli F, Mussini N, Salvatore W. Influence of shear studs distribution on the mechanical behaviour of dissipative hybrid steel frames with r.c. infill walls. Bull Earthq Eng 2019;17:957–83.
[5] Morelli F, Piscini A, Salvatore W. Development of an asymmetric re-centering dissipative device. J Constr Steel Res 2019;161:227–43.
[6] Panzera I, Morelli F, Salvatore W. Seismic multi-level optimization of dissipative re-centering systems. Earthq Struct 2020;18(1):129–45.
[7] Directive (EU) 2018 of the European Parliament and of the Council of 30 May 2018 amending Directive 2010/31/EU on the energy performance of buildings and Directive 2012/27/EU on energy efficiency 17.
[8] European Commission. The European green Deal - Communication from the Commission to the European Parliament, the European Council, the Council, the European Economic and Social Committee and the Committee of the Regions. European Commission, 12. Brussels; 2019.
[9] Pohoryles DA, Maduta C, Bournas DA, Kouris LA. Energy performance of existing residential buildings in Europe: a novel approach combining energy with seismic retrofitting. Energy Build 2020;223:110024.
[10] United Nations Environment Programme. Global status report for buildings and construction: towards a Zero-Emission. Effic Resilient Build Constr Sect, U Nations Environ Program 2020.
[11] Pohoryles DA, Bournas DA, Da Porto F, Caprino A, Santarsiero G, Triantafillou T. Integrated seismic and energy retrofitting of existing buildings: a state-of-the-art review. J Build Eng 2022;61:105274.
[12] Bournas DA. Concurrent seismic and energy retrofitting of RC and masonry building envelopes using inorganic textile-based composites combined with insulation materials: a new concept. Compos Part B 2018;148:166–79.

[13] Borri A, Corradi M, Sisti R, Buratti C, Belloni E, Moretti E. Masonry wall panels retrofitted with thermal-insulating GFRP-reinforced jacketing. Mater Struct 2016; 49:3957–68.

[14] Baek E, Pohoryles DA, Kallioras S, Bournas DA, Choi H, Kim T. Innovative seismic and energy retrofitting of wall envelopes using prefabricated textile-reinforced concrete panels with an embedded capillary tube system. Eng Struct 2022;265: 114453.

[15] Facconi L, Lucchini SS, Minelli F, Grassi B, Pilotelli M, Plizzari GA. Innovative method for seismic and energy retrofitting of masonry buildings. Sustainability 2021;13:6350.

[16] Longo F, Cascardi A, Lassandro P, Aiello MA. Thermal and Seismic Capacity Improvements for Masonry Building Heritage: a unified retrofitting system. Sustainability 2021;13:1111.

[17] Gkournelos PD, Triantafillou TC, Bournas DA. Integrated structural and energy retrofitting of masonry walls. Eff -Plane Damage Out–Plane Response J Compos Constr 2022. 04020049-2.

[18] Pertile V, De Stefani L, Scotta R. Development and characterization of a system for the seismic and energy retrofit of existing buildings. Procedia Struct Integr 2018; 11:347–54.

[19] Pertile V, Stella A, De Stefani L. Seismic and energy integrated retrofitting of existing buildings with an innovative ICF-based system: design principles and case studies. Sustainability 2021;13:9363.

[20] Valluzzi MR, Saler E, Vignato A, Salvalaggio M, Croatto G, Dorigatti G, et al. Nested buildings: an innovative strategy for the integrated seismic and energy retrofit of existing masonry buildings with CLT panels. Sustainability 2021;13:1188.

[21] Martelli L, Restuccia L, Ferro GA. The exoskeleton technology as a solution to seismic adjustment of existing buildings. Procedia Struct Integr 2020;26:175–86.

[22] Technical Report Eucentre "Valutazione della Risposta Sismica di Pannelli in blocco cassero in argilla espansa e calcestruzzo debolmente armato: il sistema BioPlus Paver". Prot. EUC324/2011U, 2011 (in Italian).

[23] Linee Guida, 2011. Linee Guida per sistemi costruttivi a pannelli portanti basati sull'impiego di blocchi cassero e calcestruzzo debolmente armato gettato in opera (in Italian).

[24] EN 1992–1-1:2005, 2005. Eurocode 2 (Annex C) - Design of concrete structures - Part 1–1: General rules and rules for building.

[25] EN 1998–1:2005, 2005 Eurocode 8: Design of structures for earthquake resistance - Part 1: General rules, seismic actions and rules for buildings, CEN - European Committee for Standardization.

[26] Circ. n°7, 2019. Istruzioni per l'applicazione dell'Aggiornamento delle "Norme tecniche per le costruzioni" di cui al decreto ministeriale 17 gennaio 2018. GU Serie Generale n.35 del 11–02-2019 - Suppl. Ordinario n. 5 (in Italian).

[27] D.M 17/01/2018. Norme Tecniche per le Costruzioni (in Italian).

[28] Paulay T, Priestley MJN. Seismic Design of Reinforced Concrete and Masonry Buildings. John Wiley & Sons, Inc,; 1992.

[29] EN 1992–4:2018 Eurocode 2 - Design of concrete structures - Part 4: Design of fastenings for use in concrete.

[30] European Convention for Constructional Steelwork, ECCS. Tech Comm 1, Et al Recomm Test Proced Assess Behav Struct Steel Elem Cycl loads 1986.

[31] Takayanagi T, Schnobrich WC. Non-linear analysis of coupled wall system. Earthq Eng Struct Dyn 1979;7.

[32] Orakcal K, Wallace JW, Conte JP. Flexural modeling of reinforced concrete walls-model attributes. Struct J 2004;101(5):688–98.

[33] Fishinger M, Rejec K, Isaković T. Modeling inelastic shear response of RC walls. Proceedings of the 15th World Conference on Earthquake Engineering. Lisbon Port 2012.

[34] Panagiotus M, Restrepo JI, Schoettler M, Geonwoo K. Nonlinear cyclic truss model for reinforced concrete walls. Acids Struct J 2012;109(S19):205–14.

[35] Mazzoni S., McKenna F., Scott M.H., et al. Opensees command Language Manual, 2007.

[36] Popovics S. A numerical approach to the complete stress-strain curve of concrete. Cem Concr Res 1973;3(5):583–99.

[37] Karsan ID, Jirsa JO. Behav Concr Compress Load J Struct Div ASCE 1969;95(12): 2535–63.

[38] Bruneau M, Uang C, Whittaker A. Ductile design of steel structures. McGraw Hill; 1998.